Regulatory Mechanisms in Biosystems

ISSN 2519-8521 (Print)
ISSN 2520-2588 (Online)
Regul. Mech. Biosyst.

Therapeutic potential of secondary metabolites of *Pleurotus ostreatus* with cardiovascular disease-related receptors through *in-silico* methods

L. J. Hernandez, E. F. Flores, S. A. Laja, H. A. Gonzaga, S. M. Firmacion, C. Ibus, L. M. Lat, E. A. Cano

Far Eastern University, Manila, Philippines

Article info

Received 01.02.2025
Received in revised form 09.03.2025
Accepted 17.04.2025

Department of Medical Technology, Institute of Health Sciences and Nursing, Far Eastern University, Manila, 1015, Metro Manila, Philippines. Tel.: 287-77-73-38. E-mail: marketing@feu.edu.ph, ihsn@feu.edu.ph, medtech@feu.edu.ph

Hernandez, L. J., Flores, E. F., Laja, S. A., Gonzaga, H. A., Firmacion, S. M., Ibus, C., Lat, L. M., & Cano, E. A. (2025). Therapeutic potential of secondary metabolites of Pleurotus ostreatus with cardiovascular disease-related receptors through in-silico methods. Regulatory Mechanisms in Biosystems, 16(2), e25044. doi:10.15421/0225044

Cardiovascular diseases (CVDs) remain the leading cause of mortality worldwide. In the search for safer therapeutic alternatives, natural products have sparked pharmaceutical interest. *Pleurotus ostreatus* (oyster mushroom), which has been reported to improve glucose and lipid metabolism, blood pressure, and appetite, is a source of essential nutrients found on hardwood trees containing medicinal bioactive compounds such as lovastatin, 9,12-octadecadienoic acid, stigmasta-5,22-dien-3-ol, and gamma-sitosterol. This study investigated the therapeutic potential of secondary metabolites of *P. ostreatus* through *in-silico* methods. Molecular docking studies and visualization were performed using PyRx and BIOVIA Discovery Studio 2024, respectively, while Absorption, Distribution, Metabolism, Excretion, and Toxicity (ADMET) profiling was conducted using ADMET 3.0 LAB and SwissAdme to assess the pharmacokinetic properties of the compounds. Furthermore, the study employed lovastatin as the reference drug for determining the favorable characteristics of the other phytochemicals. The averaged receptor-ligand complexes demonstrated that stigmasta-5,22-dien-3-ol delineated the strongest binding interaction (–8.74 kcal/mol) with the cardiovascular receptors, followed by gamma-sitosterol (–8.40 kcal/mol), lovastatin (–8.13 kcal/mol), and 9,12-octadecadienoic acid (–6.0 kcal/mol). Surpassing lovastatin in terms of binding affinities, stigmasta-5,22-dien-3-ol, and gamma-sitosterol significantly demonstrated potential inhibitory effects in the overall regulation of cardiovascular function. ADMET profiling showed lovastatin to have the most balanced profile. Although stigmasta-5,22-dien-3-ol and gamma-sitosterol demonstrated high plasma protein binding affinity and strong lipid solubility, it still required pharmacokinetic optimization to overcome poor absorption and rapid clearance. Concurrently, 9,12-octadecadienoic acid indicated outstanding biosystemic availability, although its use requires prolonged systemic caution. The findings of molecular docking coupled with ADMET analysis suggest *P. ostreatus* could potentially provide natural therapeutics for hypertension, dyslipidemia, and metabolic syndrome, warranting further exploration and confirmation for efficacy and safety.

Keywords: 9,12-octadecadienoic acid; ADMET analysis; gamma-sitosterol; molecular docking; *Pleurotus ostreatus*.

Introduction

The World Health Organization (2021) defines cardiovascular disease (CVD) as a common term used for a wide range of conditions affecting the cardiovascular system, including angina, myocardial infarction, and heart failure. Many of these conditions stem from coronary heart disease (CAD), caused by a decrease in myocardial perfusion (Shao et al., 2020). CVD is the leading cause of mortality in Asia (Zhao, 2021) and is the cause of one-third of all global deaths (Di Cesare et al., 2024). Despite advances in medical interventions, current therapeutic options are often accompanied by significant side effects and limitations, emphasizing the need for safer alternatives. Natural products have gained attention as a source of bioactive compounds with potential applications in managing various diseases (Wangchuk, 2018), and this encompasses cardiovascular diseases. Recent studies have shown that secondary metabolites, such as flavonoids, carotenoids, and glucosinolates, from plants, fungi, and other organisms, help reduce blood pressure, enhance lipid profiles, and have anti-inflammatory effects (Alum, 2024).

Pleurotus ostreatus, commonly known as oyster mushroom, is valued both as an ingredient and as a source of essential nutrients and medicinal bioactive compounds (Kadam et al., 2022). Its bioactive profile includes a variety of compounds that promote its therapeutic potential and health benefits as it functions to lower blood glucose and lipid levels (Zhao et al., 2024). The bioactive components present in *P. ostreatus* comprise phenolic compounds, glycoproteins, triterpenoids, and lipids, which have demonstrated antioxidant, anti-hypertensive, hypocholesterolemic, and anti-inflammatory activities (Waktola & Temesgen, 2020). Additionally, this mushroom is rich in primary and secondary metabolites, vitamins (including C, B_{12}, niacin, riboflavin, and thiamin), and essential fatty acids like oleic and linolenic acids, contributing to its cholesterol-lowering properties (Piska et al., 2017). However, the precise molecular mechanisms underlying these effects, particularly their interactions with cardiovascular-related receptors, remain underexplored.

An *in-silico* approach, particularly molecular docking simulations, provides a tool for investigating the molecular binding characteristics of *P. ostreatus*' bioactive compounds with target receptors. These simulations can offer insights into the structural and chemical properties of compounds that contribute to stable receptor interactions. Moreover, by focusing on the secondary metabolites of *P. ostreatus*, this study seeks to assess their molecular binding characteristics, examine structural features critical for receptor interaction stability, and identify lead compounds with high receptor-binding affinity profiles, all of which will contribute to the understanding of natural product-based treatments for cardiovascular diseases.

Materials and methods

Ligand Set Up. NCBI PubChem was employed to download the 3D structures of the secondary metabolites in SDF format. Subsequently, PyRx was utilized for its included OpenBabel feature for converting the SDF into a PDBQT format. The selected ligands utilized in the study are 9,12-octadecadienoic acid, stigmasta-5,22-dien-3-ol, gamma-sitosterol, and lovastatin.

Receptor Set Up. The study employed the following cardiovascular receptors: maltase-glucoamylase, angiotensin-converting enzyme, beta-2 adrenergic receptor, glucocorticoid, HMG-CoA reductase, insulin receptor, mineralocorticoid receptor, and peroxisome proliferator-activated receptor alpha, and angiotensin II type 1 receptor. RCSB Protein Data Bank was utilized to retrieve the 3D structure of cardiovascular receptors in a PDB format. Subsequently, BIOVIA Disco-

very Studio 2024 was used to visualize the structures for water molecules and non-relevant ligand removal, addition of polar hydrogen atoms, and receptor structure optimization.

Molecular docking. Molecular dockings were conducted through PyRx, a software particularly chosen from its multiple-ligand binding capacity simulations coupled with the binding affinities and RMSD output.

Binding affinity analysis. Incorporating Gibbs free energy into the assessment of binding strength between a receptor and a ligand is essential for understanding the mechanisms of the interaction. The degree of ΔG negativity impacts the stability of a protein-ligand complex or a ligand's binding affinity to an acceptor (Du et al., 2016). Therefore, a negative ΔG value indicates a favorable binding interaction. Likewise, a positive ΔG suggests that the binding is unfavorable. PyRx calculated a binding affinity score for each ligand-receptor complex it evaluates. This is reported in kcal/mol and reflects the strength of the interaction (Jimenez & Benitez, 2024). Similarly, Gibbs free energy, a more negative score indicates a stronger predicted binding affinity.

Pharmacokinetic profile. This process evaluated the drug potential of *P. ostreatus* secondary metabolites with cardiovascular diseases using ADMET studies. Through OpenBabel, the PDB structure of the secondary metabolites was converted to SMILES (Simplified Molecular Input Entry System). Subsequently, they were uploaded to SwissAdme and ADMET LAB 3.0 for assessing the pharmacokinetic and toxicological profile of *Pleurotus ostreatus'* secondary metabolites under the parameters of absorption, distribution, metabolism, excretion, and toxicity.

Results

Molecular docking

Angiotensin II type 1 receptor (4ZUD)

Among the tested compounds, stigmasta-5,22-dien-3-ol exhibited the strongest binding affinity (–10.2 kcal/mol), closely followed by gamma-sitosterol at –10.1 kcal/mol (Table 1). Both of these compounds demonstrated stronger binding than lovastatin at –8.7 kcal/mol, suggesting potential inhibitory effects on angiotensin II receptor activity. Meanwhile, 9,12-octadecadienoic acid showed the weakest binding affinity among the secondary metabolites of *P. ostreatus* docked (–6.7 kcal/mol).

Table 1
Docking results of human angiotensin receptor with the four secondary metabolites found in *Pleurotus ostreatus*

Ligand	Binding affinity, kcal/mol	RMSD, upper bound	RMSD, lower bound
4zud_3931_uff_E=81.58	–6.7	0	0
4zud_457801_uff_E=593.71	–10.1	0	0
4zud_5280794_uff_E=546.19	–10.2	0	0
4zud_53232_uff_E=334.51	–8.7	0	0

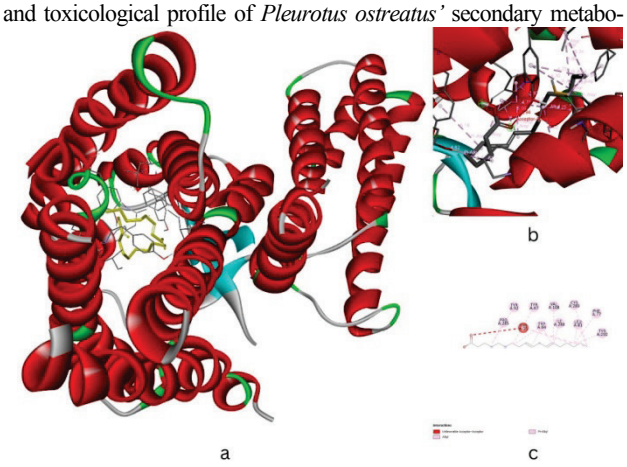

4ZUD- 3931

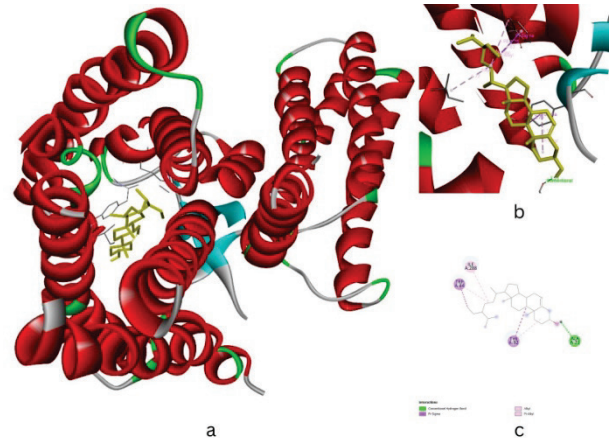

4ZUD- 457801

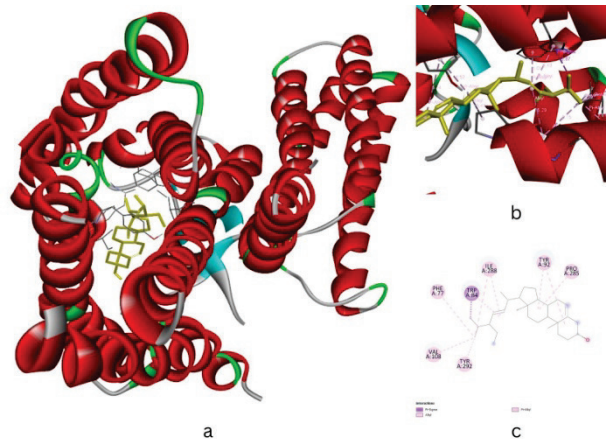

4ZUD 5280794

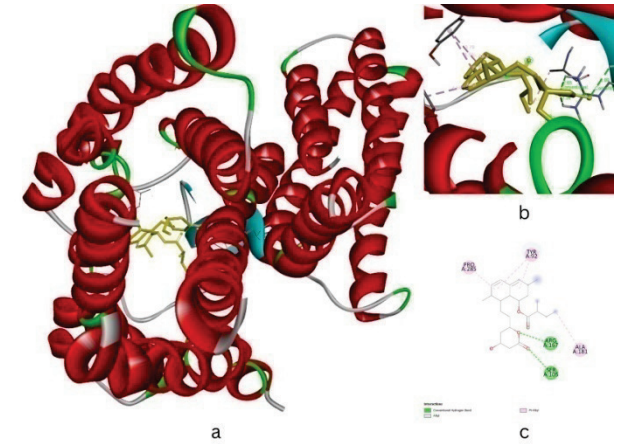

4ZUD- 53232

Fig. 1. Receptor-ligand 3D molecular visualization (*a*), ligand interactions showing bond types and distance (*b*), receptor-ligand 2D interaction (*c*)

Angiotensin II type 1 receptor (4zud) with phytochemicals of *Pleurotus ostreatus* (3931, 457801, 5280794, 53232)

Amino acid residues at specific positions and distances from angiotensin II type 1 receptor interacting with 9,12-octadecadienoic acid are entirely hydrophobic with alkyl types from VAL108 (4.25 Å), PRO205 (4.52Å), ILE288 (5.40 Å), LEU81 (4.89 Å, 5.24 Å), CYS289 (4.47 Å) and pi-alkyl types from TYR35 (4.30 Å, 4.23 Å), PHE77 (4.85 Å), TRP84 (5.00 Å, 3.97 Å, 5.41 Å, 4.10 Å, 4.79 Å,), TYR87 (5.19 Å), TYR92 (4.62 Å), and TYR 292 (4.70 Å) (Fig. 1).

Conspicuously, an amino acid residue from the receptor demonstrated an unfavorable acceptor-acceptor interaction at TYR35. Similarly, amino acids from the cardiovascular receptor interacting with gamma-sitosterol are primarily hydrophobic with TYR92 (3.75 Å, 5.15Å) and TRP84 (3.75 Å, 4.89 Å, 4.63 Å), both having pi-sigma and pi-alkyl types, ILE288 (4.72 Å) with an alkyl type, and with ALA21:O (2.21 Å) possessing conventional hydrogen bonds. Meanwhile, amino acid residues from 4zud interacting with stigmasta-5,22-dien-3-ol are entirely hydrophobic with alkyl types from PRO285 (5.48 Å), ILE288 (5.29 Å), VAL108 (3.56 Å), pi-alkyl types from TYR92 (4.51 Å, 5.43 Å) and TYR 292 (3.81 Å), and TRP84 (3.87 Å, 4.42 Å, 4.01 Å) possessing both types pi-sigma and pi-alkyl. In contrast, lovastatin demonstrates conventional hydrogen bonding from SER105:HG (2.89 Å), ARG167:HH12 (2.65 Å), and ARG167:HH2 (2.24 Å). Hydrophobic bonds are shown with alkyl types from ALA181 (4.15 Å) and PRO285 (4.58 Å) and a pi-alkyl type from TYR92 (3.79 Å, 4.84 Å).

Maltase-glucoamylase (3L4X)

Docking of the maltase-glucoamylase, an alpha-glucosidase enzyme, with four ligands from the *P. ostreatus*, resulted in varying binding affinity values (Table 2). Stigmasta-5,22-dien-3-ol with –9.4 kcal/mol demonstrated the strongest binding affinity among the compounds, and is followed by gamma-sitosterol's –8.3 kcal/mol, both of which surpass lovastatin's –7.8 kcal/mol. These greater binding affinities suggest potential inhibitory effects to maltase-glucoamylase. Meanwhile, 9,12-octadecadienoic acid binding affinity of –5.8 kcal/mol showed the weakest binding affinity among the docked phytochemicals.

Table 2
Docking results of maltase-glucoamylase (MGAM) with the four secondary metabolites found in *Pleurotus ostreatus*

Ligand	Binding affinity, kcal/mol	RMSD, upper bound	RMSD, lower bound
3l4x_3931_uff_E=81.58	–5.8	0	0
3l4x_457801_uff_E=593.71	–8.3	0	0
3l4x_5280794_uff_E=546.19	–9.4	0	0
3l4x_53232_uff_E=334.51	–7.8	0	0

MGAM (3L4X) with phytochemicals of *Pleurotus ostreatus* (3931, 5280794, 457801, 53232)

Figure 2 showcases the docking between MGAM and 9,12-octadecadienoic acid. Multiple alkyl and pi-alkyl interactions were identified between the ligand and the nonpolar amino acid residues of MGAM, such as TYR299, TRP406, PHE575, ILE328, ALA576, and ILE364. Furthermore, van der Waals forces were observed between the ligand and various residues of MGAM, including ARG526, ASP443, ASP327, GLN603, TYR605, GLY603, ASP542, THR205, THR204, and ASP203.The binding affinity between MGAM and 9,12-octadecadienoic acid is -5.8 kcal/mol, which is the lowest value among the four ligands docked with MGAM (Table 4).

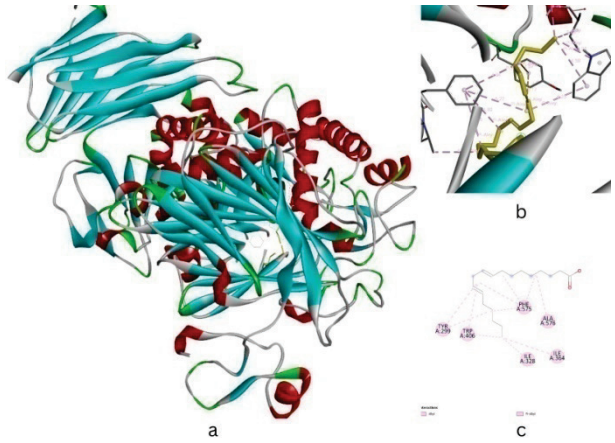

3L4X- 3931

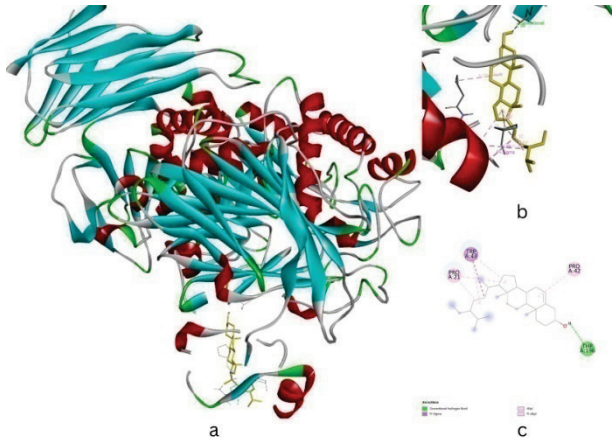

3L4X- 457801

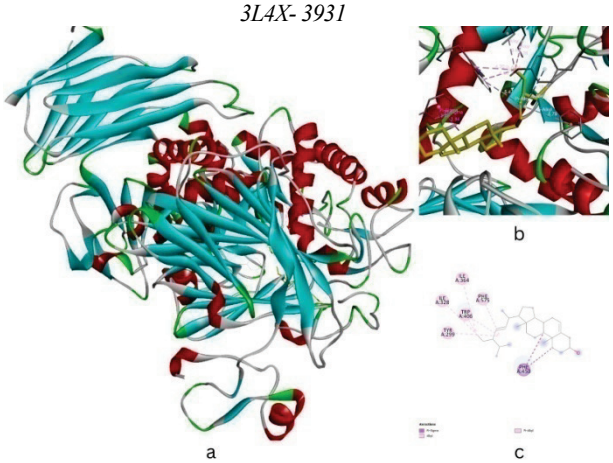

3L4X- 5280794

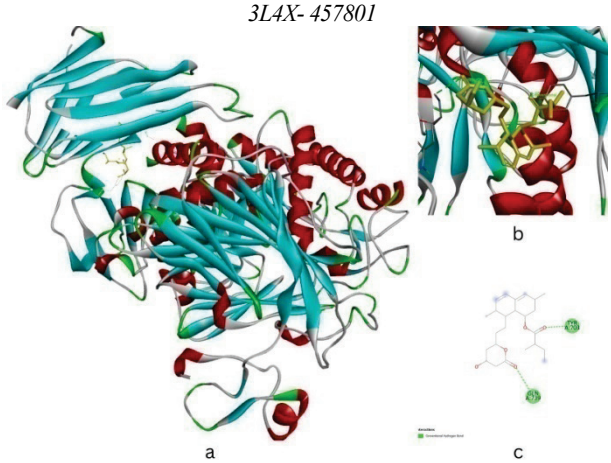

3L4X- 53232

Fig. 2. Receptor-ligand 3D molecular visualization (*a*), ligand interactions showing bond types and distance (*b*), receptor-ligand 2D interaction, when MGAM bonded to the ligands (*c*)

Several alkyl and pi-alkyl interactions were detected between the hydrophobic residues of MGAM and stigmasta-5,22-dien-3-ol, including those between ILE328, TYR299, ILE364, TRP406, and PHE575 (Fig. 2). Additionally, van der Waals interactions were also observed between the ligand and the ASP443, TRP439, ASP327, ASP542, ARG526, ASP203, HIS600, TRP441, and LYS480 residues of MGAM. Lastly, a pi-sigma interaction was identified between stigmasta-5,22-dien-3-ol and the TRP406 residue of MGAM,

indicating a covalent bond between the pi electron and a sigma bond. The binding affinity between MGAM and stigmasta-5,22-dien-3-ol is –9.4 kcal/mol, the highest among the four metabolites from *P. ostreatus*.

A conventional hydrogen bond was observed between gamma-sitosterol and the THR196 amino acid residue of MGAM (Fig. 2). Alkyl and pi-alkyl bonds were also observed between gamma-sitosterol and the PRO21 and PRO42 residues. Additionally, van der Waals forces were observed in PRO20, ARG471, SER40, VAL41, TRP194, VAL244, LYS195, ASN14, and LEU245. A pi-sigma bond interaction was also noted between gamma-sitosterol and the TRP43 residue. The binding affinity between MGAM and gamma-sitosterol is –8.3 kcal/mol, ranking second amongst the phytochemicals of *P. ostreatus* (Table 4).

Few conventional hydrogen bonds were observed between lovastatin and the TYR703 and GLN739 amino acid residues of MGAM (Fig. 2). Additionally, van der Waals forces were observed in the amino acid residues PRO740, ASN814, GLU815, LEU752, PRO751, GLY753, GLN738, THE737, LYS817, ILE755, THR632, ILE629, and GLU704. The binding of affinity of MGAM and lovastatin is –7.8 kcal/mol, which is lower than that of gamma-sitosterol (–8.3 kcal/mol) and stigmasta-5,22-dien-3-ol (–9.4 kcal/mol).

Beta-2 adrenergic receptor (2R4R)

Among the tested compounds, stigmasta-5,22-dien-3-ol delineated the strongest binding interaction with –9.5 kcal/mol, followed by gamma-sitosterol's –9.0 kcal/mol (Table 3). Both phytochemicals of *P. ostreatus* surpass lovastatin's –7.0 kcal/mol, suggesting potential inhibitory effects to ADRB2. Inconsequentially, 9,12-octadecadienoic acid binding affinity of –6.5 kcal/mol displayed the weakest binding interaction.

Table 3
Docking results of beta-2 adrenergic receptor (ADRB2) with the four secondary metabolites found in *Pleurotus ostreatus*

Ligand	Binding affinity, kcal/mol	RMSD, upper bound	RMSD, lower bound
2r4r_3931_uff_E=81.58	–6.5	0	0
2r4r_457801_uff_E=593.71	–9.0	0	0
2r4r_5280794_uff_E=546.19	–9.5	0	0
2r4r_53232_uff_E=334.51	–7.0	0	0

Beta-2 adrenergic receptor (2R4R) with the phytochemicals of *Pleurotus ostreatus* (3931, 5280794, 457801, 53232)

Figure 3 illustrates the interaction between beta-2 adrenergic receptor (ADRB2) and 9,12-octadecadienoic acid. The ligand shows a conventional hydrogen bond with the amino acid VAL54. The interaction also yielded alkyl bonds LEU275, ALA271, PRO330, ILE72, ALA335, ALA57, and an pi alkyl bond PHE336. In addition, in the interaction between the ligand gamma-sitosterol and beta-2 adrenergic receptor, diverse bonds are present, but none are new; the docking yielded alkyl bonds ILE153, LEU145, VAL126, VAL129, PRO211, VAL160, VAL157 and notably, a pi-sigma in PHE133.

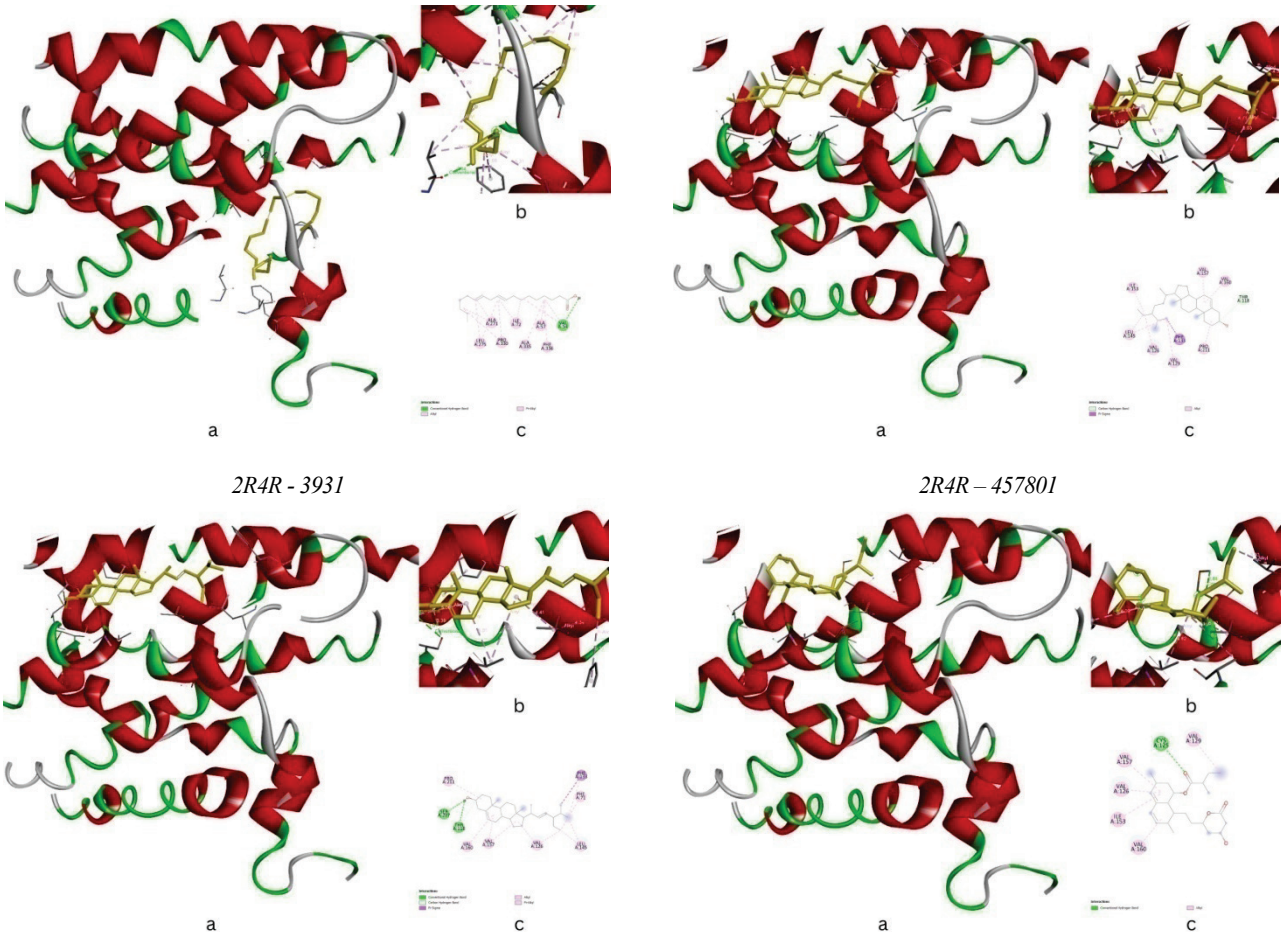

Fig. 3. Receptor-ligand 3D molecular visualization (*a*), ligand interactions showing bond types and distance (*b*), receptor-ligand 2D interaction, when ADRB2 (2R4R) bonded to the ligands (*c*)

Van der Waals bonds are also observable: PHE71, ASP120, VAL206, SER207, THR164, SER161, THR118, GLU122, CYS125. Carbon hydrogen bonds are also present fused with other bands such as the alkyl bond of the leucine (Leu) at position A:145, van der Waals bond in cysteine (Cys) at position A:125, et cetera. The binding affinity of ADRB2 and gamma-sitosterol is –9.0 kcal/mol, a value lower than the interaction of ADRB2 and 9,12-octadecadienoic acid. The interaction of ADRB2 with stigmasta-5,22-dien-3-ol shows

various bonds with the receptor. Alkyl and pi-alkyl bonds are present in the interaction with PRO211, VAL160, VAL157, VAL126, LEU125, and PHE71, and a pi-sigma bond at PHE133. Numerous van der Waals bonds are also present with THR164, SER161, GLU122, ASP130, VAL129, CYS125, VAL206. Carbon hydrogen bonds are also present. This interaction also produced two key conventional hydrogen bonds between the ligand and receptor as seen in the bonding of serine (Ser) and threonine (Thr) in positions A:207 and A118, respectively. The interaction of serine with the ligand exhibited a 2.53 Å bond length and threonine with 3.01Å as bond length. Certain notable bonds are seen within the ligand-receptor interaction of lovastatin and ADRB2, respectively. Alkyl bonds are formed with VAL129, VAL157, VAL126, ILE153, and VAL160. MET156, GLU122, SER207, PRO211, VAL210, VAL206, THR118 are present with weak, noncovalent Van der Waals. A conventional hydrogen bond also exists in this ligand-receptor interaction with cysteine (Cys) at position A:125.

Angiotensin-converting enzyme (1O8A)

The docking of the angiotensin-converting enzyme with the four ligands from *P. ostreatus* is shown in Table 6. Among the agonists, stigmasta-5,22-dien-3-ol and gamma-sitosterol demonstrated the strongest binding affinity with –9.9 and –9.3 kcal/mol, respectively. Both of these compounds surpass lovastatin's –9.2 kcal/mol, suggesting potential inhibitory effects to ACE. Conversely, 9,12-octadecadienoic acid exhibited the weakest binding affinity, indicating insignificant effects.

Table 4
Docking results of angiotensin-converting enzyme (ACE) with the four secondary metabolites found in *Pleurotus ostreatus*

Ligand	Binding affinity, kcal/mol	RMSD, upper bound	RMSD, lower bound
1o8a_5280794_uff_E=546.19	-9.9	0	0
1o8a_457801_uff_E=593.71	-9.3	0	0
1o8a_53232_uff_E=334.51	-9.2	0	0
1o8a_3931_uff_E=81.58	-5.9	0	0

Angiotensin-converting enzyme (1O8A) with phytochemicals of *Pleurotus ostreatus* (3931, 5280794, 457801, 53232)

Figure 4 showcases the docking between ACE and 9,12-octadecadienoic acid. A conventional hydrogen bond was observed between 9,12-octadecadienoic acid and the LYS118 amino acid residue of ACE, while a pi-sigma bond was observed at TRP59. Various hydrophobic bonds, such as alkyl and pi-alkyl bonds, were present at the amino acid residues TYR360, ALA63, TYR62, ILE88, and TRP357. Lastly, van der Waals forces were observed between the ligand and the THR92, ARG124, GLU123, ASP121, ALA125, TYR51, VAL119, LEU122, ASN66, and ASP358 of ACE. Hydrophobic bonds such as alkyl and pi-alkyl bonds were present between stigmasta-5,22-dien-3-ol and the nonpolar amino acid residues of ACE. Specifically, these included HIS513, HIS353, VAL518, LEU81, LEU139, and LEU140. A hydrogen bond was observed in the ASN85 residue of ACE.

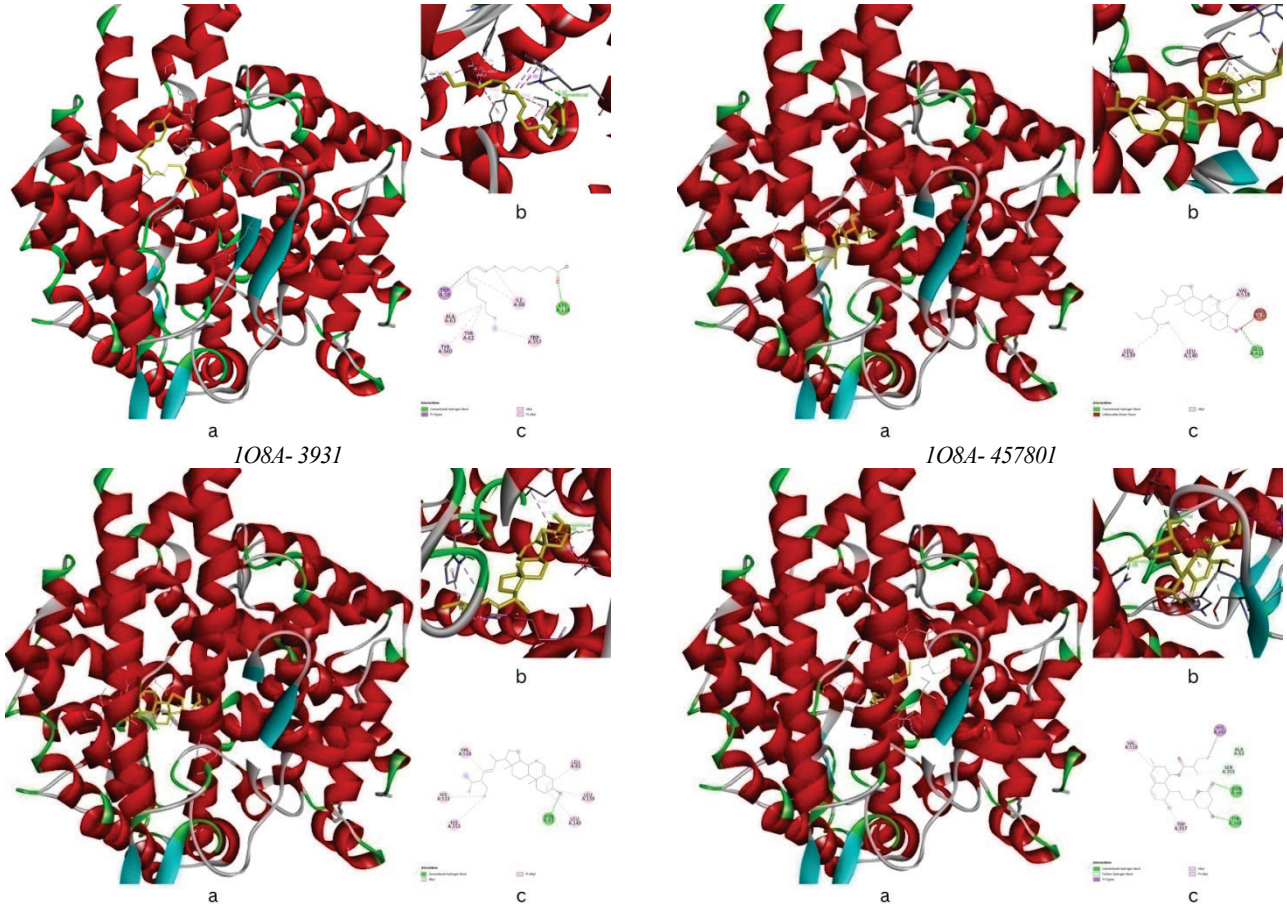

Fig. 4. Receptor-ligand 3D molecular visualization (*a*), ligand interactions showing bond types and distance (*b*), receptor-ligand 2D interaction, when ACE(1O8A) bonded to the ligands (*c*)

Van der Waals forces were observed in the following amino acid residues of the enzyme: TRP357, LYS368, VAL351, ASN66, TYR62, SER355, ARG124, PHE512, ASN70, ARG522, ALA354, SER516, GLU143, TYR69, ASN136, TYR523, and LEU82. Among these residues, LYS368, ARG124, ARG522 are positively charged (basic) while GLU143 was negatively charged (acidic). Meanwhile, ASN66, ASN70, ASN136, SER355, SER516, TYR62, TYR69, and TYR523 are polar but uncharged residues, containing polar side chains without a formal charge.

A conventional hydrogen bond was also observed between gamma-sitosterol and ACE's GLU411 amino acid residue, indicating a strong electrostatic interaction (Fig. 4). Critically, an unfavorable do-

nor-donor bond was present between the ligand and the Arg522 residue. Alkyl bonds were present at the LEU139, LEU140, and VAL518 residues of ACE, which help anchor gamma-sitosterol through hydrophobic associations. Lastly, van der Waals forces were located at the VAL351, TYR69, ASN70, ASN66, SER516, GLU143, LEU81, PHE512, ARG124, TRP356, ASN136, ASN85, SER355, and TYR523 residues. Gamma-sitosterol has the second highest binding affinity amongst the four ligands with the binding energy of –9.3 kcal/mol.

Alkyl and pi-alkyl bonds were present between lovastatin and ACE residues VAL518 and TRP357, contributing to hydrophobic stabilization within the binding pocket (Fig. 4). Conventional hydrogen bonds were spotted at the ASN66 and TYR360 residues, reinforcing the ligand's affinity for ACE through electrostatic interactions. Lastly, van der Waals forces were observed in the following ACE amino acid residues: ALA354, TYR523, PHE391, HIS410, ARG522, ALA63, HIS353, ALA356, SER355, GLU411, PHE512, TYR62, LYS368, VAL351, ASN70, ASP358, which further supports the stability of the protein-ligand complex. The binding affinity between lovastatin and ACE was calculated to be –9.2 kcal/mol, ranking third among the four *P. ostreatus*-derived ligands (Table 4).

Glucocorticoid (1M2Z)

Among the tested ligands, lovastatin exhibited the strongest affinity at –7.3 kcal/mol. and is followed closely by stigmasta-5,22-dien-3-ol at –7.2 kcal/mol (Table 5). The nearly parallel strong binding affinity of stigmasta-5,22-dien-3-ol with lovastatin suggests potential activating or inhibiting effects to glucocorticoid. Moreover, despite the near values of gamma-sitosterol and 9,12-octadecadienoic with the other two compounds, their respective binding scores of 6.8 and –6.4 kcal/mol still indicate weak binding interactions.

Table 5
Docking results of glucocorticoids (1M2Z)
with the four secondary metabolites found in *Pleurotus ostreatus*

Ligand	Binding affinity, kcal/mol	RMSD, upper bound	RMSD, lower bound
2znn_3931_uff_E=81.58	–6.4	0	0
2znn_457801_uff_E=593.71	–6.8	0	0
2znn_5280794_uff_E=546.19	–7.2	0	0
2znn_53232_uff_E=334.51	–7.3	0	0

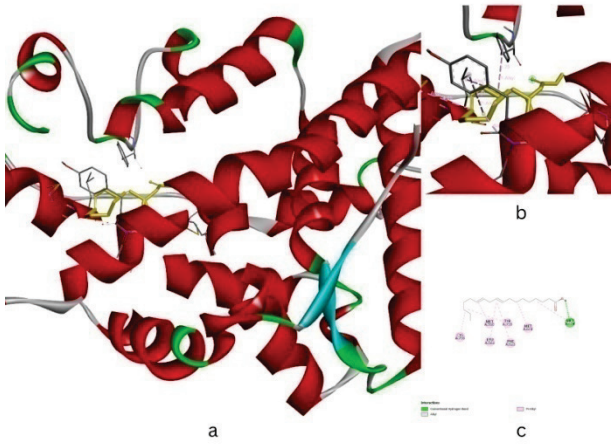

1M2Z- 3931

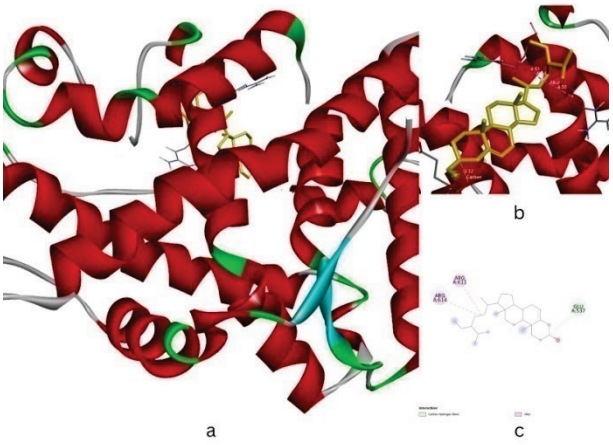

1M2Z- 457801

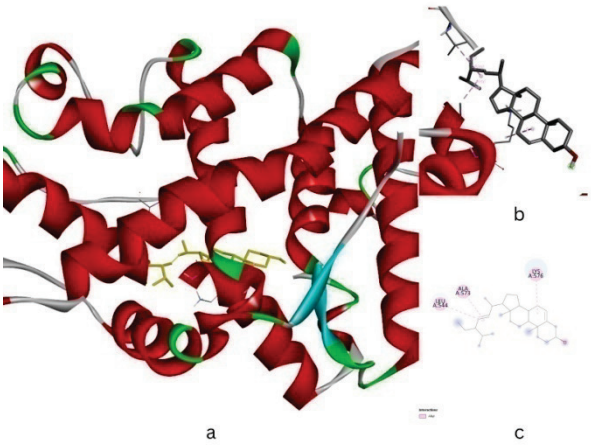

1M2Z- 5280794

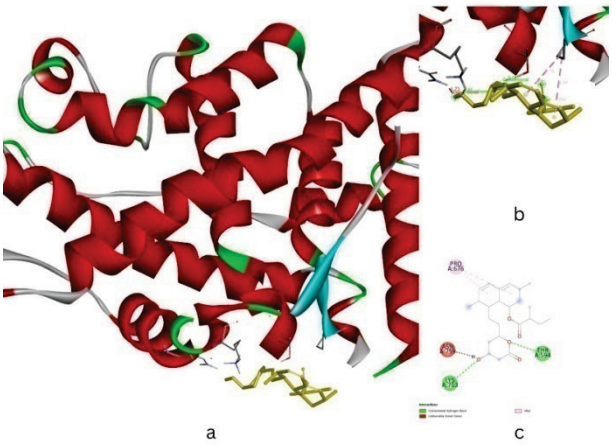

1M2Z- 53232

Fig. 5. Receptor-ligand 3D molecular visualization (*a*), ligand interactions showing bond types and distance (*b*), receptor-ligand 2D interaction, when glucocorticoids (1m2z) bonded to the ligands (*c*)

Glucocorticoid (1M2Z) with phytochemicals of *Pleurotus ostreatus* (3931, 5280794, 457801, 53232)

Figure 5 shows the important key interactions between glucocorticoid and 9,12-octadecadienoic acid, such as the conventional hydrogen bond formed at MET604 residue In addition to hydrogen bonds, the docking reveals hydrophobic interactions, including alkyl and pi-alkyl interactions. Contributing to alkyl interactions are the CYS736, LEU563, MET560, and MET601, while residues PHE623 and TYR735 participate in pi-alkyl interactions. The binding affinity of glucocorticoid and 9,12-octadecadienoic acid is –6.4 kcal/mol, the lowest among the four ligands that were docked (Table 5). Furthermore, the binding of gamma-sitosterol and the glucocorticoid receptor formed a conventional hydrogen bond at residue GLU537. Additionally, alkyl interactions were also present in ARG611 and ARG614 residues. Meanwhile, van der Waals interactions were observed in the following amino acid residues of the enzymes: GLN615, GLU540, GLU542, PRO625, TRP610, TYR660, and VAL543. The resulting binding affinity of gamma-sitosterol with the glucocorticoid receptor is measured at –6.8 kcal/mol.

In contrast to the first two ligands, the docking of glucocorticoid and stigmasta-5,22-dien-3-ol only created van der Waals and hydro-

phobic (alkyl) interactions. Alkyl interactions were present in ALA573, LEU544, and LYS576 residues while van der Waals interactions were observed between the ligand and ALA580, ARG569, GLU542, ILE539, ILE572, PRO541, TRP577, and VAL538 residues. The binding affinity of stigmasta-5,22-dien-3-ol with the glucocorticoid receptor is –7.2 kcal/mol, which is stronger compared to the first two ligands (Table 5).

Van de Waals, hydrogen bonds, hydrophobic bonds (Alkyl), and unfavorable donor-donor interaction, were revealed in the docking of glucocorticoid and lovastatin. Alkyl interaction was seen between the ligand and PRO676 residue. On the other hand, hydrogen bonds were present at LYS763 and THR594. Moreover, van der Waals interactions were created on the following amino acid residues: ASN768, ASP590, ASP591, ASP678, GLN597, GLN760, GLY679, LEU680, LYS677, LYS681, MET593, and TYR598. Lastly, an unfavorable donor-donor interaction was created and was present at ASN759. Among the four ligands docked with glucocorticoid, lovastatin created the highest binding affinity at –7.3 kcal/mol (Table 5).

HMG-CoA reductase (1DQ9)

Table 6 summarizes the binding affinities of HMG-CoA reductase with the compounds of *P. ostreatus*. The docking score indicates gamma-sitosterol (457801), stigmasta-5,22-dien-3-ol (5280794), and lovastatin (53232) to have almost analogous binding affinities. The strong binding affinities of gamma-sitosterol with –7.8 kcal/mol and stigmasta-5,22-dien-3-ol with a –7.4 kcal/mol surpassing lovastatin's –7.3 kcal/mol suggest potential inhibitory effects to HMG-CoA reductase. On the contrary, 9,12-octadecadienoic acid (3931) exhibited the weakest binding affinity, suggesting a non-relevant role with HMG-CoA reductase.

Table 6
Docking results of HMG-CoA Reductase (IDQ9)
with the four secondary metabolites found in *Pleurotus ostreatus*

Ligand	Binding affinity, kcal/mol	RMSD, upper bound	RMSD, lower bound
1dq9_3931_uff_E=81.58	–4.9	0	0
1dq9_53232_uff_E=334.51	–7.3	0	0
1dq9_457801_uff_E=593.71	–7.8	0	0
1dq9_5280794_uff_E=546.19	–7.4	0	0

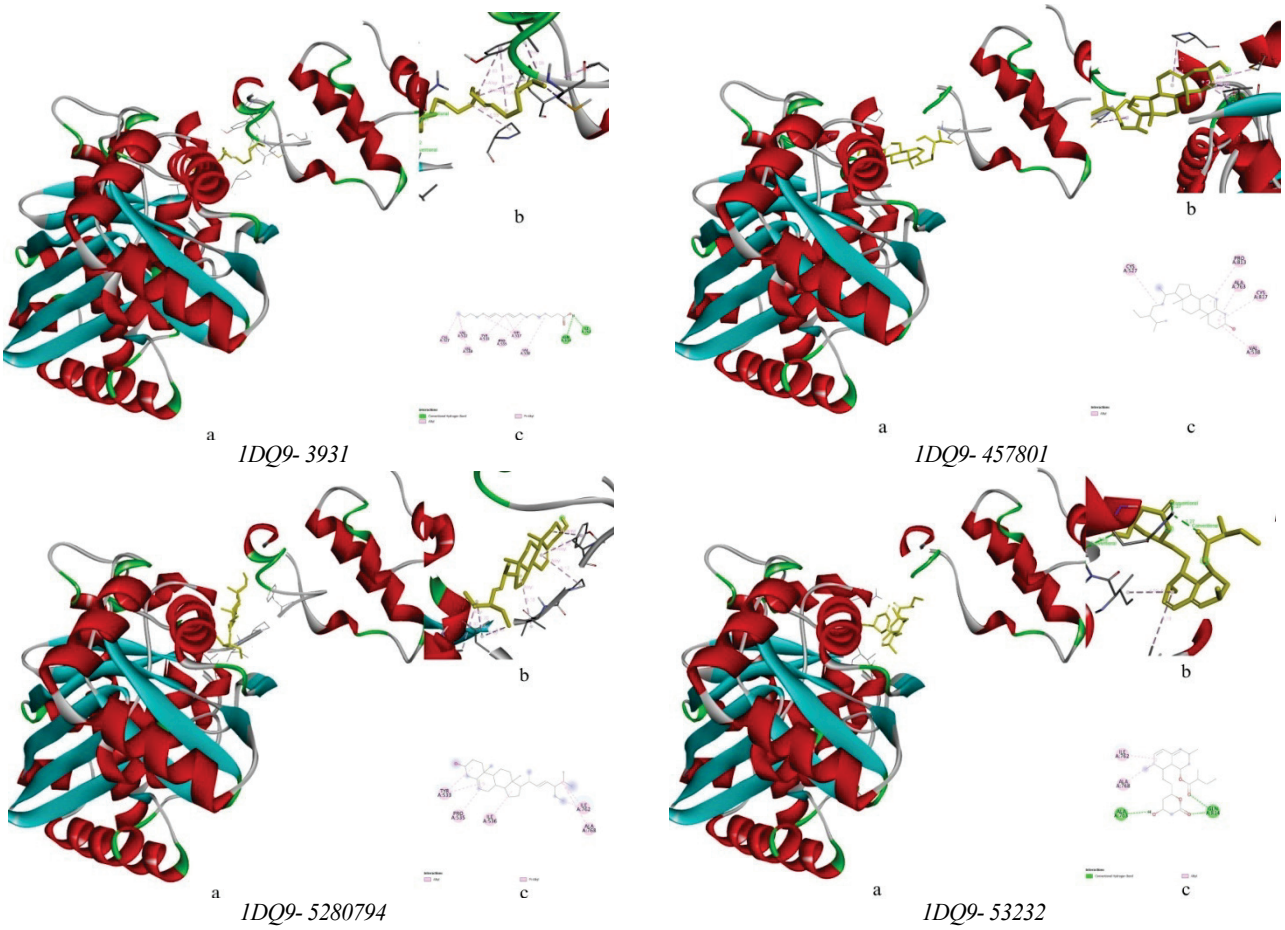

Fig. 6. Receptor-ligand 3D molecular visualization (*a*), ligand interactions showing bond types and distance (*b*), receptor-ligand 2D interaction, when HMG-CoA reductase (1DQ9) bonded to the ligands (*c*)

HMG-CoA reductase (1DQ9) with phytochemicals of *Pleurotus ostreatus* (3931, 5280794, 457801, 53232)

Figure 6 shows the interaction of 9,12-octadecadienoic acid (Pubchem ID: 3931) with HMG-CoA reductase (1DQ9). Conventional hydrogen bond interactions are present in glutamine (Gln) located at position 814 and isoleucine (Ile) located at 762,which significantly contributes to the conformation energy and indicates a stronger effect on complex formation. Van der Waals interactions are seen with GLY532, GLY765, TYR519, MET534, PRO813, ILE536. This interaction refers to a non-polar force of attraction that binds between molecules when atoms are near each other. Hydrophobic interactions (Alkyl and Pi-alkyl) are CYS527, VAL522, VAL530, VAL538, TYR533, TYR517 and PRO535.

Van der Waals are present in MET534, TYR533, TYR519, TYR517, CYS526, LEU811, VAL522, VAL530, GLY532, ILE536, GLN814, and ALA556 of HMG-CoA reductase and gamma-sitosterol. Pi-alkyl interactions are present in CYS527, CYS817, PRO813, ALA763 and VAL538, respectively.

HMG-CoA reductase with stigmasta-5,22-dien-3-ol has van der Waals interactions seen in TYR517, TYR761, PRO813, GLN814, GLN766, GLY765, and MET534, respectively while hydrophobic interactions such as alkyl and pi-alkyl are present in TYR533, PRO535, ILE536, ILE762, and ALA768. This interaction is the strongest out of

all the ligands that were docked as it is lower than –7.0 kcal/mol. HMG-CoA reductase with lovastatin shows conventional hydrogen bonds in ALA763 and GLN814 that contribute to the conformational energy of the ligand. Moreover, alkyl interactions are present in ILE762 and ALA768, respectively. van der Waals interactions are present in ALA556, ILE536, GLN766, GLY808, CYS526, CYS527, TYR533, TYR517, VAL522, LEU811, MET534, and PRO813. Hydrogen bonds and hydrophobic bonds interaction contribute to the specificity of the ligand , which suggests that it binds strongly to HMG-CoA reductase.

Mineralocorticoid receptor (1YA3)

Amongst the phytochemicals of *P. ostreatus*, stigmasta-5,22-dien-3-ol and gamma-sitosterol demonstrated the strongest binding affinity with –9.2 and –9.0 kcal/mol), respectively (Table 7). Exhibiting superior binding affinities to lovastatin with –8.1 kcal/mol, these compounds suggest potential inhibitory effects to the mineralocorticoid receptor. Ultimately, 9,12-octadecadienoic acid showed the weakest binding affinity with a –6.7 kcal/mol.

Table 7
Docking results of mineralocorticoid receptor (1YA3) with the four secondary metabolites found in *Pleurotus ostreatus*

Ligand	Binding affinity, kcal/mol	RMSD, upper bound	RMSD, lower bound
1ya3_3931_uff_E=81.58	-6.3	0	0
1ya3_457801_uff_E=593.71	-9.0	0	0
1ya3_5280794_uff_E=546.19	-9.2	0	0
1ya3_53232_uff_E=334.51	-8.1	0	0

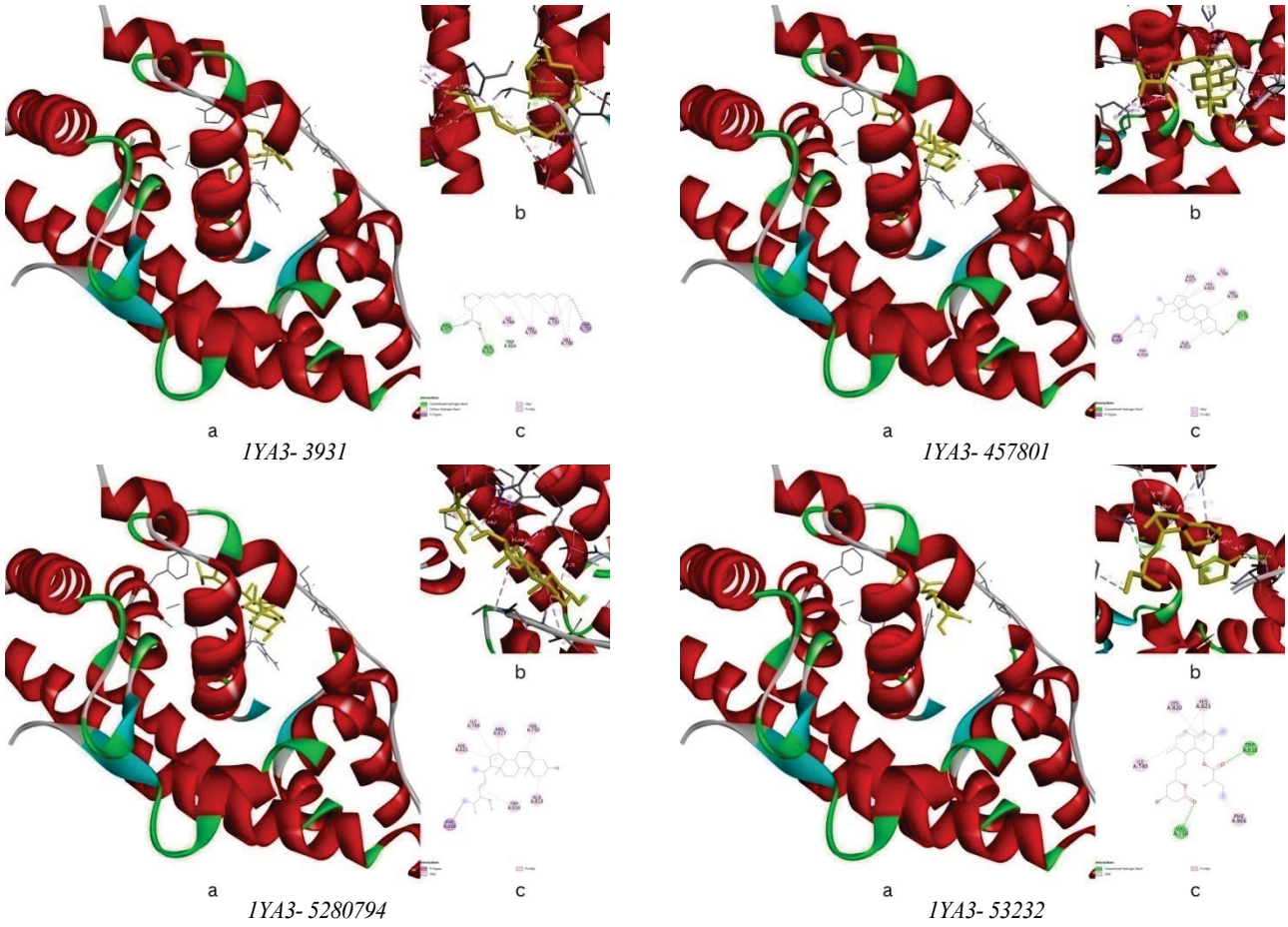

Fig. 7. Receptor-ligand 3D molecular visualization (*a*), ligand interactions showing bond types and distance (*b*), receptor-ligand 2D interaction, when 1ya3 are bonded to the ligands (*c*)

The 9,12-octadecadienoic acid forms hydrogen bonds and hydrophobic interactions with critical mineralocorticoid residues, suggesting potential modulatory effects on the receptor. The hydrogen bond is formed between the ligand and ARG817 and ALA813 residues, which help in the stability of the complex. Multiple alkyl and pi-alkyl interactions are observed between the ligand and hydrophobic residues such as ILE749, PRO747, TRP783, TRP816, VAL750, and VAL780, which contribute to the ligand's binding affinity by anchoring it in the receptor's hydrophobic pocket. A pi-sigma interaction contributes to the ligand's stability within the binding site and potentially influences the receptor's conformational changes. This complex shows a binding affinity of –6.3 kcal/mol, indicating a relatively weak interaction compared to other ligands that may bind more strongly to the receptor.

For stigmasta-5,22-dien-3-ol, the hydrophobic interactions of alkyl and pi-alkyl that stabilize the ligand-receptor complex through van der Waals forces are observed with the following residues: ALA813, VAL750, ILE749, and LEU810. These hydrophobic interactions are important for binding within the receptor's active site. The polar bonding that provides further stabilization are notable to GLN776, GLU746, and ARG817. The close proximity of key receptor residues to the ligand atoms signifies the complementarity of the ligand to the binding pocket of mineralocorticoid. Stigmasta-5,22-dien-3-ol has shown the highest affinity to mineralocorticoid receptors with –9.2 kcal/mol affinity with zero RMSD values.

The gamma-sitosterol demonstrates various interactions such as hydrophobic interactions, hydrogen bonding, and Van der Waals forces. The hydrophobic bonds of PHE866 and ALA813 observed from alkyl and pi-alkyl interaction contribute to the hydrophobic nature of gamma-sitosterol binding. In addition, a hydrogen bond is observed between gamma-sitosterol and GLN776, which also stabilizes the binding. Furthermore, particular residues such as VAL780 and MET777 provide additional stabilization through van der Waals forces. The interaction between the mineralocorticoid receptor (MR) and the lovastatin are stabilized by interactions such as hydrogen binding, hydrophobic interactions, van der Waals forces, and amino acid residues.

The hydrophobic interactions that further stabilize the interaction are found between the ligand and amino acid residues. Alkyl and pi-alkyl interactions are present, enhancing ligand binding through non-polar contacts. Residues such as PHE866 and PRO747 contribute to hydrophobic interactions. The Mineralocorticoid Receptor (MR) and the ligand lovastatin have a binding affinity of –8.1 kcal/mol indicating a relatively moderate interaction.

Peroxisome proliferator-activated receptor (PPAR-a) (2ZNN)

Table 8 demonstrates the binding strength of the four secondary metabolites of *P. ostreatus* with PPAR-α. Lovastatin demonstrated the strongest binding affinity with –9.0 kcal/mol, followed by gamma-sitosterol with –8.1 kcal/mol, stigmasta-5,22-dien-3-ol with –7.0 kcal/mol, and 9,12-octadecadienoic acid with a –6.7 kcal/mol docking score. The strong receptor-ligand complex with gamma-sitosterol, only second to lovastatin, potentially suggest activating effects to PPAR-α.

Table 8
Docking results of peroxisome proliferator-activated receptor (PPAR-a) (2ZNN) with the four secondary metabolites found in *P. ostreatus*

Ligand	Binding affinity, kcal/mol	RMSD (upper bound)	RMSD (lower bound)
2znn_3931_uff_E = 81.58	–6.5	0	0
2znn_457801_uff_E = 593.71	–8.1	0	0
2znn_5280794_uff_E= 546.19	–7.0	0	0
2znn_53232_uff_E = 334.51	–9.0	0	0

Figure 8 displays the interaction between the PPAR-a receptor and 9,12-octadecadienoic acid. Alkyl bonds were found in ILE272, MET330, LEU247, VAL324, ILE339, CYS275, ALA333, and VAL332. However, a singular conventional hydrogen bond was displayed in TYR334. Amino acid residues from PPAR-a receptor interacting with 9,12-octadecadienoic acid showed the predominance of alkyl hydrophobic bonds: ILE272, MET330, LEU247, VAL324, VAL332, ILE241, ILE339, ILE247, CYS275, and ALA333.

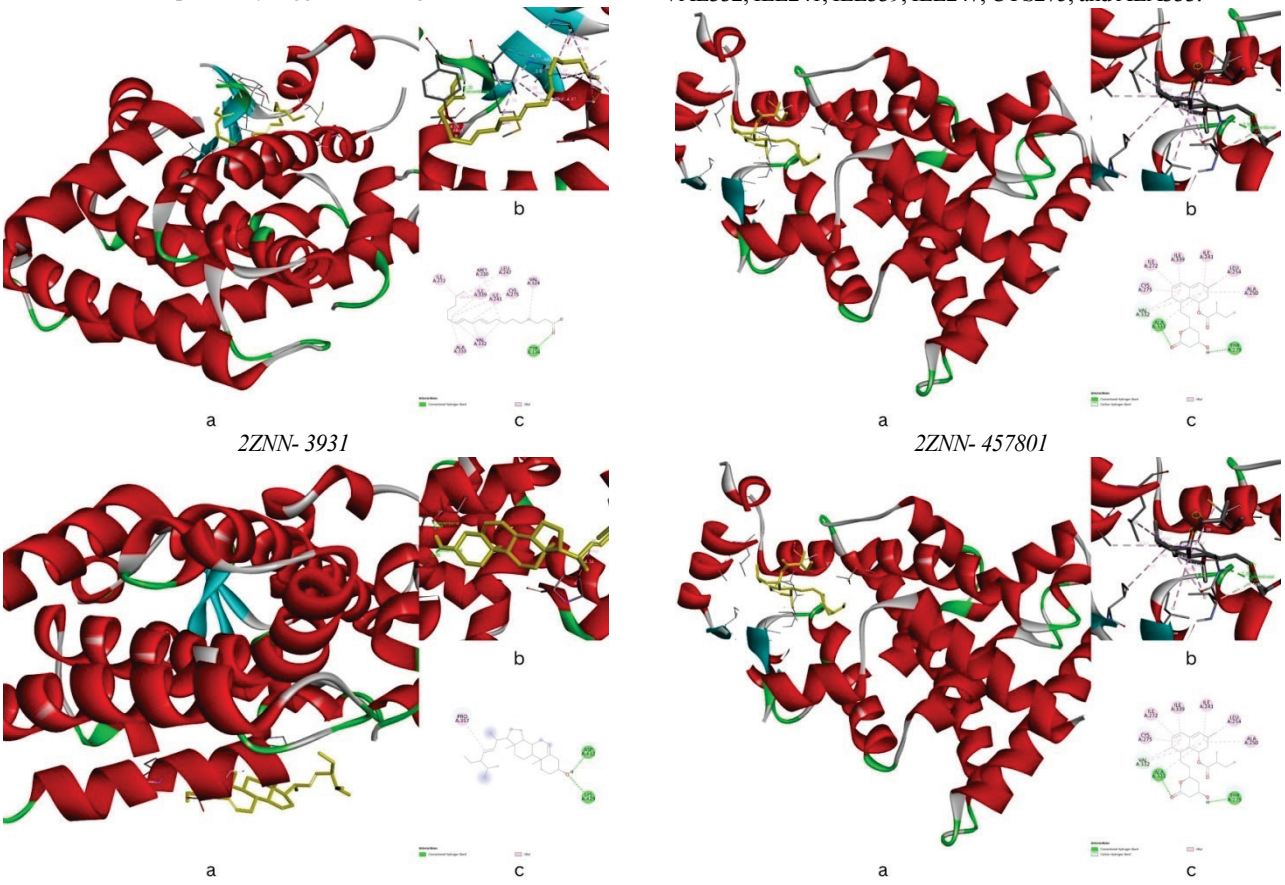

Fig. 8. Receptor-ligand 3D molecular visualization (*a*), ligand interactions showing bond types and distance (*b*), receptor-ligand 2D interaction, when PPAR-a (2znn) bonded to the ligands (*c*)

Concurrently, a singular conventional hydrogen bond can also be seen at TYR334 (Fig. 8). On the other hand, the receptor with stigmasta-5,22-dien-3-ol are primarily conventional hydrogen bonds with ASP432 and LYS429 while a single hydrophobic bond with an alkyl type can be observed at PRO357. Meanwhile, the interaction between the PPAR-α receptor and gamma-sitosterol highlighted the presence of only hydrophobic bonds of alkyl types from VAL255, CYS275, VAL332, CYS276, LEU321, and ILE 339. Lastly, PPAR-a receptor with lovastatin produced various interactions from alkyl hydrophobic bonds in CYS275, ILE272, ILE339, ILE241, LEU254, and ALA250 to conventional hydrogen bonds in ALA333 and THR279, and hydrogen bonds in CYS275, VAL332, ALA333, and THR279.

Insulin receptor (4IBM)

Table 9 illustrates the binding affinity and RMSD values of the four secondary metabolites of *P. ostreatus* with the insulin receptor. Stigmasta-5,22-dien-3-ol demonstrated the strongest binding affinity with –8.5 kcal/mol, followed by lovastatin with –7.8 kcal/mol. Gamma-sitosterol exhibited a slightly parallel binding affinity with lovastatin with a –7.6 kcal/mol docking score. These stronger and almost parallel binding affinities suggest potential activating effects on the insulin receptor. Among the tested compounds, 9,12-octadecadienoic acid showed the weakest binding affinity with a –6.7 kcal/mol docking score.

Insulin receptor (4IBM) with phytochemicals of *Pleurotus ostreatus* (3931, 5280794, 457801, 53232)

The interaction between insulin receptor (IR) and 9,12-octadecadienoic acid shows van der Waals bonds in ASN1224, GLN1217, GLN1211, LEU1228, and PRO1231. There is a conventional hydrogen bond in the amino acid residue tryptophan at position 1200. An alkyl bond with LEU1213, LYS1220, and a pi-alkyl bond

TYR1210, a Pi-sigma bond can also be found in PHE1221, and an unfavorable interaction (acceptor-acceptor) in ASP1229. The docking of the gamma-sitosterol with the receptor produced numerous bonds that exhibited van der Waals interaction such as SER1086, ASN1097, TYR1087, ASP1083, HIS1081, GLY1082, LEU1002, MET1076, LYS1030, ILE1157, and GLY1003.

Table 9
Docking results of insulin receptor (4IBM)
with the four secondary metabolites found in *Pleurotus ostreatus*

Ligand	Binding affinity, kcal/mol	RMSD, upper bound	RMSD, lower bound
4ibm_3931_uff_E=81.58	–5.3	0	0
4ibm_457801_uff_E=593.71	–7.6	0	0
4ibm_5280794_uff_E=546.19	–8.5	0	0
4ibm_53232_uff_E=334.51	–7.8	0	0

Further adding to the van der Waals interactions present, there is a conventional hydrogen bond with aspartate at position 1150. Moreover, alkyls are also present in VAL1010, MET1139, MET1153, and ALA1028. The docking of IR and stigmasta-5,22-dien-3-ol had van der Waals interactions such as SER1086, SER1090, ASN1097, TYR1087, HIS1081, ALA1080, ASP1083, LEU1002, GLY1082, MET1076, ALA1028, ASP1150, LYS1030, GLY1005, GLN1004, and GLY1003. Three alkyl bond residues are found in ILE1157, MET1139, and VAL1010, and an unfavorable bump in MET1153. The ligand-receptor simulation between lovastatin and IR resulted in copious van der Waals interactions with SER1090, TYR1087, ALA1028, LEU1078, GLY1082, MET1079, LEU1002, VAL1010, MET1139, THR1154, ASP1083, GLY1003, MET1163, GLN1004, and GLY1005, an alkyl bond in ILE1157, a carbon hydrogen bond with SER1086 and a conventional hydrogen bond with an amino acid residue asparagine in position 1097, and an unfavorable acceptor-acceptor in HIS1081.

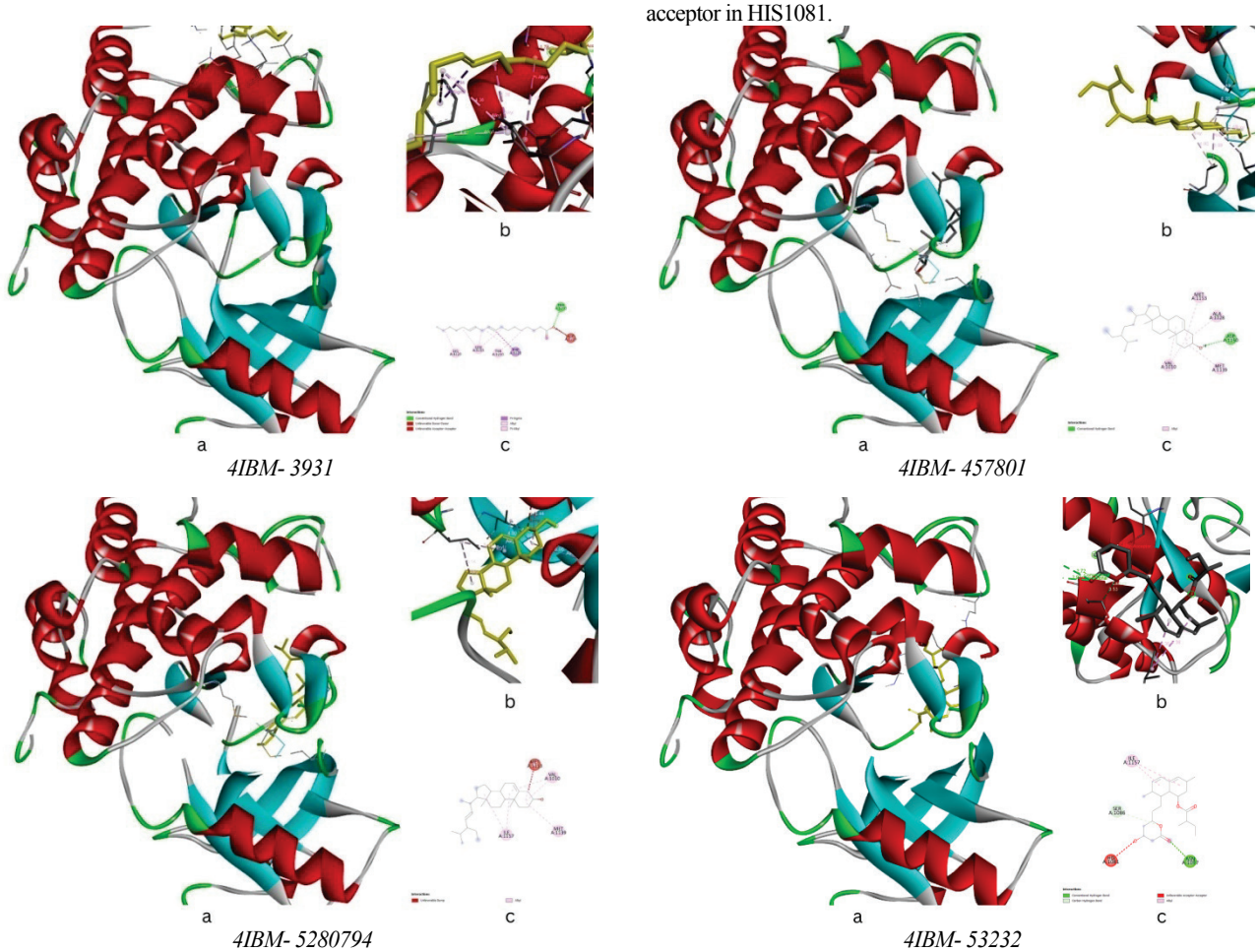

Fig. 9. Receptor-ligand 3D molecular visualization (*a*), ligand interactions showing bond types and distance (*b*), receptor-ligand 2D interaction, when insulin receptor (4IBM) bonded to the ligands (*c*)

RMSD Values. The selected cardiovascular related receptors docked with the chosen phytochemicals of *Pleurotus ostreatus* demonstrate RMSD values of 0.0 Å (Table 1–9).

ADMET analysis

All compounds exhibited high molecular weights and lipophilic tendencies, with logP values exceeding 5 for most compounds (Table 10).

Absorption and distribution

Table 11 demonstrates high gastrointestinal absorption from 9,12-octadecadienoic acid and lovastatin. In contrast, gamma-sitosterol and stigmasta-5, 22-dien-3-ol show a lower GI absorption. Meanwhile, gamma-sitosterol, 9,12-octadecadienoic acid, and lovastatin exhibited high plasma protein binding of 98.64%, 96.96%, and 91.72% respectively. On the other hand, stigmasta-5,22-dien-3-ol exhibits moderate to low PPB of 86.31%.

Metabolism and excretion

The metabolic result demonstrates that gamma-sitosterol, lovastatin, and stigmasta-5,22-dien-3-ol are CYP3A4 substrates (Table 12). Conversely, 9,12-octadecadienoic acid differs, stipulating its conformance to an alternative metabolic pathway. Additionally, the human liver microsomal stability shows instability to gamma-sitosterol and stigmasta-5,22-dien-3-ol while conversely, compelling 9,12-octadecadienoic acid and lovastatin with stability. Furthermore, 9,12-octadecadienoic acid exhibited the lowest clearance rate with 3.80 mL/min/kg. On the other hand, lovastatin delineated moderate clearance with 8.23 mL/ min/kg while gamma-sitosterol and stigmasta-5,22-dien-3-ol demonstrated rapid clearance of 12.68 and 13.92 mL/min/kg, respectively.

Table 10
Physicochemical properties of the phytochemicals of *Pleurotus ostreatus*

Property	Optimal range	Gamma-sitosterol (457801)	9,12-Octadecadienoic acid (3931)	Lovastatin (53232)	Stigmasta-5,22-dien-3-ol (5280794)
Molecular weight, g/mol	100–600	414.39	280.24	404.26	412.37
Hydrogen bond acceptors	0–12	1	2	5	1
Hydrogen bond donors	0–7	1	1	1	1
Topological Polar Surface Area (TPSA)	0–140	20.23	37.3	72.83	20.23
LogP (Lipophilicity)	≤5	7.85	6.83	4.56	6.57
Aqueous Solubility (LogS)	≥–4	–6.95	–5.42	–4.82	–5.73
Bioavailability score	≥0.55	0.988	0.149	0.999	0.964

Table 11
Absorption and distribution properties of the selected phytochemicals of *Pleurotus ostreatus*

Property	Gamma-sitosterol (457801)	9,12-Octadecadienoic acid (3931)	Lovastatin (53232)	Stigmasta-5, 22-dien-3-ol (5280794)
GI Absorption	low	high	high	low
Plasma protein binding (PPB), %	98.64	96.96	91.72	86.31
Blood-brain barrier (BBB) permeability	no	no	no	no

Table 12
Metabolism and excretion properties of the selected phytochemicals of *Pleurotus ostreatus*

Metabolism property	Gamma-sitosterol	9,12-Octadeca-dienoic acid	Lovastatin	Stigmasta-5,22-dien-3-ol
CYP3A4 Substrate	yes	no	yes	yes
CYP3A4 Inhibitor	no	no	yes	no
Human liver microsomal stability	unstable	stable	stable	unstable
Clearance,mL/min/kg	12.68	3.80	8.23	13.92
Half-life, hours	short	long	moderate	short

Toxicity prediction

Inhibition of the human Ether-à-go-go-Related Gene (hERG) is demonstrated low for all the compounds (Table 13). Although gamma-sitosterol, lovastatin, and stigmasta-5,22-dien-3-ol demonstrated the risk for hepatocellular toxicity. 9,12-octadecadienoic acid, on the other hand, did not exhibit the hepatotoxicity risk. Ultimately, Ames mutagenicity predicts that the selected phytochemicals are unlikely to cause direct DNA mutations.

Discussion

Reference Drug. Lovastatin is an FDA approved statin drug used on account of its lipid-lowering mechanism to treat and prevent coronary heart disease, hypercholesterolemia, and adolescent patients with heterozygous familial hypercholesterolemia (Duong & Bajaj, 2023). The therapeutic use of lovastatin occurs when metabolized in the stomach to its active form-beta-hydroxy acid through competitive inhibition of HMG-CoA reductase, a rate-limiting enzyme in cholesterol synthesis (Srivastava et al., 2019). As a result, LDL catabolism becomes augmented from the stimulation of LDL receptors on hepatocytes due to the decrease in serum cholesterol (De Denus & Spinler, 2002; Ray & Cannon, 2005). Additionally, inhibitors of HMG-CoA induce improvement of endothelial function, reduction of inflammation at coronary plaque sites, inhibition of platelet aggregation, and anticoagulant effects (Gelosa et al., 2007; Duong & Bajaj, 2023).

Table 13
Toxicity prediction of the selected phytochemicals of *P. ostreatus*

Toxicity parameter	Gamma-sitosterol	9,12-Octadeca-dienoic acid	Lova-statin	Stigmasta-5,22-dien-3-ol
hERG inhibition (cardiotoxicity)	low	low	low	low
Hepatotoxicity	yes	no	yes	yes
Ames mutagenicity	no	no	no	no

In this study, lovastatin will serve as the reference drug for assessing the therapeutic potential to CVDs in comparison with the other phytochemicals of *P. ostreatus* – 9,12-octadecadienoic acid, gamma-sitosterol, and stigmasta-5,22-dien-3-ol – by determining whether its binding affinities with cardiovascular receptors and ADMET profile will exhibit shortcoming, equivalent, or leveraging results over the other secondary metabolites.

Receptors. All the receptors are retrieved from RCSB PDB. The receptors were chosen based on the article by Hamedi et al. (2020). Table 14 shows the following receptors, together with their function complex in the cardiovascular system.

Table 14
A list of the cardiovascular disease-related receptors retrieved from RCSB PDB that were used in the study after validation

Cardiovascular disease-related receptor	PDB ID	Function
Angiotensin II Type 1 receptor	4zud	Primary blood pressure regulator and involves fluid and electrolyte homeostasis (Zhang et al., 2015).
Maltase-glucoamylase (MGAM)	3l4x	Glucose metabolism; hydrolyzes dietary polysaccharides into glucose (Wang et al., 2016). Inhibition is often done to manage hyperglycemia.
Beta-2 adrenergic receptor (ADRB2)	2r4r	Bronchodilator, vital for the management of asthma (Garzon-Siatoya et al., 2021). Decreases cardiomyocyte apoptosis (Yang et al., 2019).
Angiotensin-converting enzyme (ACE)	1o8a	Elevated levels of angiotensin II can lead to hypertension, which is why ACE inhibitors are commonly used to treat hypertension and CVDs (Messerli et al., 2018).
Glucocorticoid	1m2z	Cardioprotective and anti-inflammatory effects (Cruz-Topete et al., 2020).
HMG-CoA Reductase	1dq9	A regulatory enzyme for the biosynthesis of isoprenoids and cholesterol. Phosphorylated on Ser871 and is disabled by AMP-activated protein kinase (AMPK) in response to ATP depletion (Kemp et al., 2022).
Mineralocorticoid receptor	1ya3	Activation can promote inflammation, fibrosis, and hypertension (Nishiyama, 2018). The use of mineralocorticoid antagonists benefits patients suffering from heart failure (Jhund et al., 2024).
Peroxisome proliferator-activated receptor (PPAR-a)	2znn	Rof metabolism genes of lipoprotein. Utilizes glucose and lipids through increasing mitochondrial function (Montaigne et al., 2021).
Insulin receptor	4ibm	Mediates the effects of insulin. Involved in the tyrosine kinase activity (Tatulian, 2015). Binds insulin and is, therefore, related in the insulin-insulin receptor complex.

Ligands. The secondary metabolites of *P. ostreatus* were retrieved from PubChem, a publicly available database which houses information about various chemicals and compounds. The target ligands were selected based on the article of Mishra et al. (2022). Table 15 shows the list of the secondary metabolites primarily involved with the cardiovascular system and its diseases.

Angiotensin II type 1 receptor (4zud) with phytochemicals of *Pleurotus ostreatus* (3931, 457801, 5280794, 53232)

The binding between angiotensin II type 1 receptor and 9,12-octadecadienoic acid produced a docking score of –6.7 kcal/mol, presenting a moderate binding interaction (Table 1). Data from the docking report shows that pi-alkyl bonding is the strongest and predomi-

nant type in this interaction, followed by an alkyl bonding. These interactions contribute to the stability of the receptor-ligand complex, suggesting that the ligand has greater affinity with lipid environments. Notably, the ligand produced multiple pi-alkyl bonding from TRP84 with 4 interactions exhibiting strong distances: 5.00 Å, 3.97 Å, 4.10 Å, and 4.79 Å, in addition to the 1 moderate distance of 5.41 Å, suggesting that this is the primary force that holds the ligand in place. This finding suggests that the ligand is anchored in an aromatic-rich pocket, forming stable interactions, and is not randomly binding. Repetitive interactions with the aromatic amino acid in the receptor increases its specificity factor, inducing more stability and a higher likelihood of receptor modulation. Meanwhile, the alkyl-alkyl interactions also contribute to a stronger hydrophobic stabilization, as attributed by strong distances of amino acid residues: VAL108, PRO285, LEU81, and CYS289 and moderate distances of ILE288 and LEU81. Despite evidence of stable molecular interactions, the binding affinity remains high, affecting the interaction strength. The following data suggest that the unfavorable acceptor-acceptor interaction at TYR35 significantly affected this result, as repulsion between two electron-rich groups can destabilize the ligand's positioning.

Table 15
List of the secondary metabolites that are found in *P. ostreatus* that are involved with cardiovascular system diseases

Pleurotus ostreatus' secondary metabolites	PubChem CID	Function
9,12-Octadecadienoic acid	3931	Has an inverse relationship with coronary heart disease (CHD) (Farvid et al., 2014). When bound with an agonist, induces bronchodilation (Boora, 2023).
Gamma-sitosterol	457801	Has antihyperglycemic capabilities (Bamuragan et al., 2011); inhibits gluconeogenesis (Tripathi et al., 2013).
Stigmasta-5,22-dien-3-ol	5280784	Ameliorates glucose transporter type 4 (GLUT4) translocation and decreases insulin resistance, which decreases fasting glucose (Nualkaew et al., 2015 as cited in Bakrim et al., 2022).
Lovastatin	53232	Used to treat hypercholesterolemia and to reduce lipidemia (Xie et al., 2021). A precursor for statins which are cholesterol-lowering drugs (Wang et al., 2021).

The molecular binding between angiotensin II type 1 receptor and gamma-sitosterol shows a strong interaction from a binding affinity of –10.1 kcal/mol (Table 1). Docking reports display that a conventional hydrogen bond is the strongest interaction in this complex, which is followed by hydrophobic interactions, pi-alkyl, alkyl-alkyl, and pi-sigma. The data shows that ALA21:O is an important amino acid in the receptor with which the ligand can form strong hydrogen bonds . Additionally, the bond distance is optimal with 2.21 Å, contributing to the receptor-ligand stability. This finding also contributes to the selectivity of ligand interaction, increasing its value for therapeutic potential. Subsequent to the strong hydrogen bonds are the hydrophobic interactions including pi-alkyl, alkyl-alkyl, and pi-sigma. Collectively, these contribute to the overall stability of the receptor-ligand interaction and suggest their affinity to thrive in lipid environments with pi-sigma being the weakest, however, still contributing by fine-tuning ligand orientation with the receptor pocket. Particularly, TRP84 represents the strongest and primary amino acid interaction in the hydrophobic category with 2 pi-alkyl bonds and 1 pi-sigma bond exhibiting strong distances. Following TRP84 is TYR92 with a pi-sigma and pi-alkyl, then lastly, ILE288 with an alkyl-alkyl bonding. By consolidating these different molecular bonds, the superior binding affinities of gamma-sitosterol can be attributed by the strong conventional hydrogen bond with ALA21:O and repetitive interactions involving TRP84 and TYR92, which enhances ligand anchoring and reduces energy expenditure.

The molecular interaction between angiotensin II type 1 receptor and stigmasta-5,22-dien-3-ol delineates the strongest docking in the CVD receptor complex (10.2 kcal/mol) with the secondary metabolites of *P. ostreatus* (Table 1). Docking reports portray pi-alkyl bonds as the most significant hydrophobic bonds regarding binding sites, as TRP84 and TYR92, both with double interactions, 2 strong distances (4.42 Å, 4.01 Å) and 1 with strong (4.51 Å) and moderate distance (5.43 Å), respectively, acting as the central force of the interaction from its repetitive characteristics. This finding suggests greater stability and more specific interaction between the complex, indicating more potency for receptor modulation. The other pi-alkyl bonds include the interaction originating from PHE77 and TYR292 which exhibit moderate (5.13 Å) and strong distances (3.81 Å), respectively. Subsequently, the hydrophobic bonds in strength are followed by the alkyl bonds with only VAL108 demonstrating a good distance of 3.56 Å and PRO285 (5.47 Å) and 2 ILE288 (5.29 Å, 5.15 Å) with moderate distances. Finally, the pi-sigma bond from TRP84 is the weakest binding interaction among the mentioned interactions. Overall, the complex interaction, particularly the repetitive interactions with TRP84 and TYR92, is suggestive of stigmasta-5,22-dien-3-ol's attribute of superior binding affinity.

The molecular binding between angiotensin II type 1 receptor and lovastatin shows a strong interaction with a binding affinity of -8.7 kcal/mol. Binding interactions show that hydrogen bonds are the strongest and main constituent of the receptor-ligand interaction with SER105:HG, ARG167:HH12, and ARG167:HH22 displaying strong distances of 2.89 Å, 2.65 Å, and 2.23 Å, respectively. This data is suggestive of the lovastatin's capacity to form strong hydrogen bonds with angiotensin II type 1 receptor, implying the ligand's selectivity and proper positioning. Consequently, contributing to the stability of the interaction are the hydrophobic bonds with the stronger pi-alkyl 2 bonding from TYR92 (3.79 Å, 4.84 Å) and the alkyl-alkyl bonds from ALA181 (4.15 Å) and PRO285 (4.58 Å), all exhibiting strong distances.

MGAM (3L4X) with phytochemicals of *Pleurotus ostreatus* (3931, 5280794, 457801, 53232)

The relatively low binding affinity of 9,12-octadecadienoic acid can be attributed to its deficiency of stronger electrostatic interactions such as hydrogen or ionic bonds. Instead, it primarily engages in hydrophobic interactions such as van der Waals, alkyl, and pi-alkyl bonds. This observation aligns with the study of Yazdi et al. (2016), which suggests that the lipophilic tail of a polyunsaturated fatty acid (PUFA) engages in broader and non-specific hydrophobic interactions with the hydrophobic core of a protein, while the carboxylic head group forms fewer and more specific electrostatic interactions. As a PUFA, 9,12-octadecadienoic acid also relies on its lipophilic tail for hydrophobic interactions with MGAM, which explains its relatively lower binding affinity. These hydrophobic interactions, while crucial for thermodynamic stability, are weaker than hydrogen bonds. According to Ferenczy & Kellermayer (2022), hydrophobic contribution to protein mechanical stability ranged from one-fifth to one-third of the total force, while hydrogen bonds contributed to the rest. Nonetheless, these noncovalent interactions, while weak individually, collectively contribute to the overall binding affinity between ligand and enzyme. In particular, hydrophobic interactions are crucial for the initial recognition and binding of ligands to their receptors (Wright et al., 2023).

Similarly, the alkyl and pi-alkyl interactions suggest a strong hydrophobic association that contributes a stabilizing effect to the ligand within the binding site (Ferenczy & Kellermayer, 2022). Furthermore, non-covalent interactions, such as the van der Waals interactions, particularly in regions with polar or charged residues, contribute to the overall binding strength of the ligand-receptor complex. Although stigmasta-5,22-dien-3-ol has the lowest binding energy among the four ligands, it does not contain a hydrogen bond. Hydrogen bonding is typically considered a strong contributor to binding affinity. However, it is not the sole determinant. According to Majewski et al. (2019), structural stability is not a prerequisite for tight binding, and they reported that a quarter of analyzed complexes in their dataset lacked robust hydrogen bonds. Stigmasta-5,22-dien-3-ol's higher binding affinity can be attributed to several possible factors. Firstly, the stigmasta-5,22-dien-3-ol forms multiple alkyl and pi-alkyl interactions with the MGAM residues ILE328, TYR299, ILE364, TRP406,

and PHE575. According to Cramer et al. (2021), the burial of nonpolar surface areas during binding can enhance binding affinities through entropy or enthalpy-driven hydrophobic effects associated with such nonpolar interactions. Secondly, the protein-ligand formed in this docking has stronger van der Waals forces. The greater number of van der Waals interactions, and hydrophobic interactions in general, compensate for the absence of hydrogen bonds. Barratt et al. (2005) supports this claim, stating that dispersion interactions, such as van der Waals forces, dominate binding thermodynamics due to a lack of solvent interactions in the binding pocket. This suggests that van der Waals interactions play a significant role in stabilizing such complexes. Lastly, the pi-sigma interaction with Trp406 suggests that stigmasta-5,22-dien-3-ol engages in sigma-electron cloud interactions.

The hydrogen bond between gamma-sitosterol and the THR196 residue of MGAM introduced a strong electrostatic interaction that significantly contributed to the stability of the ligand-receptor complex. According to Sim et al. (2008), the N-terminal β-sandwich domain of the MGAM spans residues 52 to 269, which includes THR196. While this domain is not directly part of the core active site, it plays a significant role in shaping active site architecture. The formation of a hydrogen bond between gamma-sitosterol and THR196 suggests a stabilizing effect on the architecture surrounding the entrance to the active site. Furthermore, Fu et al. (2018) emphasized the critical role of hydrogen bonds in protein-ligand interactions in stabilizing the overall structure and strengthening the binding effect between protein and ligand. In addition to the conventional hydrogen bond with THR196, gamma-sitosterol also contains alkyl, pi-alkyl, and van der Waals interactions. These hydrophobic forces also contribute to the stabilization of protein and ligand, such as the MGAM and gamma-sitosterol complex (Wright et al., 2023).

Despite the relatively weaker interaction with MGAM, the presence of hydrogen bonds and van der Waals interactions suggests a meaningful affinity between MGAM and lovastatin. According to Sim et al. (2008), the proximal C-terminal domain consists of residues 652–730, including TYR703 and GLN739 which formed the hydrogen bonds with lovastatin. Similar to gamma-sitosterol, the proximal C-terminal domain does not directly contribute to the active site, but rather to the architecture supporting it (Sim et al., 2008). Its proximity to the active site suggests that the formation of hydrogen bonds with TYR703 and GLN739 influences the stability of the protein-ligand complex. According to Bulusu & Desiraju (2019), hydrogen bonds are critical to the recognition of ligands by proteins due to electrostatic nature, which allows for long-range interactions that play a key role in biomolecular recognition. These interactions also contribute to both specificity and reversibility of protein-ligand binding, ensuring that biological processes can still be regulated and dynamic. Concurrently, hydrophobic interactions in the form of van der Waals forces, contribute to the overall stability of the complex, reinforcing lovastatin's positioning within MGAM (Wright et al., 2023).

Beta-2 adrenergic receptor (2R4R) with the phytochemicals of *Pleurotus ostreatus* (3931, 5280794, 457801, 53232)

The binding affinity of ADRB2 and 9,12-octadecadienoic acid is –6.5kcal/mol. Even though there exists a conventional hydrogen bond within the interaction, one of the factors that affect binding energy is the geometry of the interaction design itself. It is observable that the interaction of ADRB2 and 9,12-octadecadienoic acid is with multiple bonds with greater than 3.5 Å of bond length. This indicates that this interaction is not as strong, as stronger interactions typically exhibit greater than –7.0 kcal/mol of binding energy. The interaction is considered moderate as weak binding energy is often associated with binding energies of less than –5.0 kcal/mol. This is because although the bond lengths are suboptimal, the quantity of the hydrogen bonds make up for this. In other words, the binding energy is reasonably stable, but not strong enough, especially for drug design, hence the necessity for more optimization. Prospective observational studies done by Farvid et al. (2014) demonstrated that dietary linoleic acid intake has an inverse relationship with coronary heart disease (CHD). 9,12-octadecadienoic acid when bound to ADRB2 activates the associated G protein which consequently activates adenylyl cyclase, increasing cyclic adenosine monophosphate, which then results in the physiological downstream signaling pathways made by the receptor's effects (bronchodilation and vasodilation) (Garzon-Siatoya et al., 2021). The physiological effect, of course, varies depending on its type (agonist or antagonist) and the receptor's location, which in this case is the blood vessels.

The binding affinity of ADRB2 and gamma-sitosterol is –9.0 kcal/mol, a value lower than the interaction of ADRB2 and 9,12-octadecadienoic acid. This indicates that it has far more favorable binding characteristics than the latter. The complex exhibits a ligand that forms a stable and energetically compatible receptor. It suggests that the ligand and receptor interact strongly, making persistence to physiological conditions more bearable, therefore, increasing its biological efficiency. As reflected by its high binding energy, it is a candidate for drug design discovery. This is supported by Balamurugan et al. (2011), who said that gamma-sitosterol increased insulin secretion in response to glucose. Moreover, the same research illustrated that gamma-sitosterol-treated rats exhibited decreased liver enzymes such as alanine aminotransaminase (ALT), aspartate aminotransaminase (AST), alkaline phosphatase (ALP), and acid phosphatase (ACP) as opposed to diabetic control rats. This suggests that gamma-sitosterol has antihyperglycemic capabilities (Bamuragan et al., 2011) and is also capable of inhibiting gluconeogenesis (Tripathi et al, 2013). Moreover, Endrini et al. (2014), stated that gamma-sitosterol induced cytotoxicity toward cancer cells of the colon and the liver. However, research by Sirikhansaeng et al. (2017), showed DNA damage in human peripheral blood mononuclear cells such as monocytes and lymphocytes only in select plants, which prompts people to consider its toxicity and the amount of consumption.

Out of the four ligands, stigmasta-5,22-dien-3-ol had the best interaction and affinity with the receptor. One of the factors that made it so is the bi-conventional hydrogen bonds with the amino acid serine and threonine, which ultimately led to an interaction with great strength and versatility. Through these conventional hydrogen bonds and their respective contributions to the stability and strength of the molecular system, it is ensured that specificity would also be present. However, the existence of a variety of alkyl, van der Waals, and hydrogen bonds in general contributes not only to the stability and rigidity of the design but also to its flexibility. Furthermore, the amino acid, PHE133, is bound to the ligand by a pi-sigma, which occurs when the electron cloud of the phenyl ring interacts with the electron density of a nearby σ-bond. This, however, is not that significant as it is mostly indicative of a weak, non-covalent bond. Vital for molecular docking and drug design is an optimal balance between such factors. Through this, drug discovery centered around this ingredient has potential for treating cardiovascular diseases.

Lovastatin and ADRB2 interacted with -7.0 binding affinity. This energy is neither high or low, however. Research shows that lovastatin is a potent secondary metabolite recovered from fungi, and it is used to treat hypercholesterolemia and to reduce lipidemia (Xie et al., 2021). Wang et al. (2021) added that lovastatin is the precursor for statins, which are again, cholesterol-lowering drugs. Interestingly, lipophilic statins possess neuroprotective benefits on animal models with Parkinson's disease (Lin et al, 2021). This connects as due to malfunctions in the autonomic nervous system, PD patients experience cardiac dysautonomia, a cardiovascular disease common in such patients, tachycardia and vasoconstriction are also common (Grosu et al., 2023; Cuenca-Bermejo et al., 2021). Moreover, cardiovascular abnormalities are often cured with the therapeutic usage of L-DOPA, which lowers blood pressure and aggravates orthostatic hypotension from unnatural causes (Cuenca-Bermejo et al., 2021). The process and underlying mechanisms of lovastatin as a substitute are not included in the scope of this research.

Angiotensin-converting enzyme (1O8A) with phytochemicals of *Pleurotus ostreatus* (3931, 5280794, 457801, 53232)

These observed interactions between ACE and 9,12-octadecadienoic acid suggested a strong hydrophobic association, contributing to

the ligand's stabilization within the active site. The presence of hydrogen bonding observed in the ASN85 residue of ACE, provided electrostatic stabilization, further reinforcing the ligand's affinity for ACE. Similarly, the discussed non-covalent interactions, particularly those with polar or charged residues, contribute to the overall stability of the ligand-receptor complex (Cramer et al., 2021).

Similar interactions were observed in the binding of ACE with stigmasta-5,22-dien-3-ol. The combination of these van der Waals forces with strong hydrophobic interactions suggests that stigmasta-5,22-dien-3-ol effectively anchors itself within the ACE binding pocket, potentially influencing its enzymatic activity and exerting a stabilizing effect.

This presence of the unfavorable donor-donor interaction at ARG522 could potentially destabilize the binding of the gamma-sitosterol to ACE, affecting its overall binding affinity and stability by introducing steric hindrance or electrostatic repulsion. According to Dhorajiwala et al. (2019), unfavorable bonds between protein-ligand complexes reduce their stability because they indicate a force of repulsion occurring between two molecules and an atom. Despite the presence of unfavorable interaction, the strong binding affinity suggests that gamma-sitosterol establishes stable interactions with the ACE binding site by having other interactions compensate for the unfavorable donor-donor interaction. For example, the presence of the hydrogen bond at the GLU411 residue of ACE influences the stabilization of the complex. According to Fu et al. (2018), hydrogen bonding plays a crucial role in stabilizing protein-ligand interactions, reinforcing the impact of the hydrogen bond between gamma-sitosterol and GLU411. Additionally, Wright et al. (2023) highlights the role of hydrophobic interactions, such as alkyl and van der Waals forces, in maintaining ligand binding stability, which further supports the interaction between gamma-sitosterol and ACE.

While slightly lower than gamma-sitosterol, lovastatin still exhibited strong binding interactions, suggesting a meaningful inhibitory potential. The presence of hydrogen bonding, along with alkyl and van der Waals interactions, further supports the stability of this complex. Bulusu & Desiraju (2019) claims that hydrogen bonds are critical for ligand recognition and binding specificity, ensuring stable yet reversible interactions. Hydrophobic bonds such as alkyl interactions also contribute to the binding affinity by driving the burial of nonpolar surface areas during binding (Cramer et al., 2021). Similarly, Barratt et al. (2005) reports that dispersion interactions, such as van der Waals forces, dominate binding thermodynamics in the binding pocket and exert a stabilizing effect.

Glucocorticoid (1M2Z) with phytochemicals of *Pleurotus ostreatus* (3931, 5280794, 457801, 53232)

The observed conventional hydrogen bonds between glucocorticoid and 9,12-octadecadienoic acid suggested an essential role in anchoring the ligand and ensuring correct orientation within the active site. Meanwhile, the discussed hydrophobic interaction,s specifically alkyl and pi-alkyl interactions, play a major role in stabilizing the ligands at the binding pocket of the receptor (Patil et al., 2010). Alkyl interactions create a hydrophobic environment that stabilizes the ligand, while pi-alkyl interactions further enhance its stability. The binding affinity of glucocorticoid and 9,12-octadecadienoic acid is the lowest among the four ligands that were docked (Table 5). Although there are hydrophobic interactions and a single hydrogen bond, the overall interaction network lacks electrostatic interaction, which is known to contribute significantly to binding strength. 9,12-Octadecadienoic acid is hydrophobic in nature, which means that its interactions are mostly weaker alkyl and pi-alkyl forces rather than strong hydrogen bonds. Moreover, the potential energetic penalty is associated with desolvating the hydrophobic ligand as it enters the binding pocket, combined with the entropy loss from the ligand adopting a more rigid conformation upon binding. Vaidyanathan et al. (2023) further added that the presence of hydrophobic interactions, such as alkyl and pi-alkyl, competes with hydrogen bonds, leading to decreased binding affinity. Similarly, the binding of gamma-sitosterol and the glucocorticoid receptor created van der Waals interaction in addition to the discussed interactions. The formation of van de Waals interactions plays a vital role in the interaction between the ligand and the receptor. The binding affinity of gamma-sitosterol with the glucocorticoid receptor is slightly higher than the binding affinity of glucocorticoid and 9,12-octadecadienoic acid. However, it is still considered to be relatively low, reflecting some factors that limit the strength of the interaction. Although a hydrogen bond is present, it is still not sufficient to achieve a high binding affinity, especially as it only exists at one residue. According to Beach et al. (2023), multiple hydrogen bonding offers a more enhanced binding efficiency than a single hydrogen bond. Moreover, the ligand relies on weak hydrophobic interactions, such as van de Waals interactions, indicating that gamma-sitosterol does not fully make use of the glucocorticoid's potential for strong hydrophobic interactions.

Despite the absence of a hydrogen bond, the interaction between glucocorticoid and gamma-sitosterol forms multiple alkyl interactions, which means that it is well-suited to the receptor's hydrophobic environment, explaining its stronger binding affinity compared to the first two ligands (Table 5). Aside from alkyl interactions, the van der Waals interactions provide sufficient stabilizing energy. According to Righetti & Boschetti (2013), these interactions are individually weak attractions, but their combined effect can strengthen the binding interaction. Thus, these features, even without a hydrogen bond, make the ligand more stable when bonding with the receptor.

The presence of unfavorable donor-donor interaction between glucocorticoid and lovastatin may imply that there is a presence of repulsive forces between the ligand and receptor (Odhar et al., 2022). Although there is a presence of unfavorable donor-donor interaction, which can weaken the overall binding affinity, other factors outweigh the negative impact of repulsion. As stated in the previous discussion, hydrogen bonds greatly stabilize binding interaction. Thus, with this receptor-ligand interaction there is a significant binding strength because two hydrogen bonds were formed. Moreover, the presence of alkyl and van der Waals interaction provide a favorable structural compatibility to the receptor's binding pocket. Overall, the combination of these forces made the lovastatin the strongest ligand and the most possible modulator of glucocorticoid receptor activity.

HMG-CoA reductase (1DQ9) with phytochemicals of *Pleurotus ostreatus* (3931, 5280794, 457801, 53232)

The conventional hydrogen bond interaction of HMG-CoA reductase and 9,12-octadecadienoic acid contributes to the conformation energy that stabilizes the binding between the ligand and its receptor. According to Wu et al. (2012), hydrogen bonds indicate that the effects of these bonds to the complex formation will be stronger, and the results will be more accurate. The geometry of interaction of Van der Waals is one of the factors that highly influence the binding energy of a ligand and receptor that includes the bond lengths and orientations.

Van der Waals interactions in HMG-CoA reductase and gamma-sitosterol are shown to have a weak and non-covalent interaction because of its dipole induced dipole attraction between molecules. With that, it is still significant in the molecular docking of HMG-CoA reductase with gamma-sitosterol as it stabilizes the ligand.

HMG-CoA reductase and stigmasta-5,22-dien-3-ol Van der Waals interactions contribute to the different interactions of proteins but due to their structural complexity, the magnitude of their effects is estimated based on molecular geometry (Roth et al., 2000). The multiple bonds further elevate their binding strength and specificity. As its binding energy indicates a strong and stable interaction, further improvements may enhance and develop its specificity and stability that may make it a potential candidate for the therapeutic approach.

Conventional hydrogen bonds which contribute to the conformational energy of the ligand, alkyl interactions and Van der Waals observe a strong and specific binding affinity between lovastatin and HMG-CoA reductase. Both hydrogen bonds and hydrophobic bonds interaction contributes to the specificity of the ligand, which suggests that it binds strongly to HMG-CoA reductase.

Mineralocorticoid receptor with phytochemicals of *Pleurotus ostreatus* (3931, 5280794, 457801, 53232)

The docking study reveals that all four secondary metabolites of *P. ostreatus* show negative binding affinities with mineralocorticoid receptors, suggesting favorable interactions. In molecular docking, lower (more negative) binding affinity values indicate a favorable and strong interaction between the ligand and protein (Uzzaman et al., 2019). Among the metabolites, the mineralocorticoid receptor demonstrates the strongest binding affinity with gamma-sitosterol, followed by stigmasta-5,22-dien-3-ol, lovastatin, and 9,12-octadecadienoic acid.

The mineralocorticoid receptor and gamma-sitosterol demonstrated the strongest binding interaction, indicating that this complex may effectively compete with aldosterone and act as an antagonist. The binding energy of –9.2 kcal/mol suggests extremely stable interaction and potentially inhibits the activation of the mineralocorticoid receptor. If such complex interactions are further confirmed experimentally, it could potentially act as a nonsteroidal MR antagonist that exhibit s anti-inflammatory and antifibrotic effects, making it a natural alternative for cardiovascular management. In addition, the second metabolite, stigmasta-5,22-dien-3-ol, also exhibited a strong binding affinity of –9.0 kcal/mol, which shows a proximity with the first metabolite in terms of inhibition mechanism. Similarly, if such metabolite is experimentally studied, this compound can potentially be used in cardiovascular management and remodeling. The lovastatin metabolite showed moderate binding affinity of –8.1 kcal/mol. Despite its weaker binding affinity, it can still be an MR antagonist candidate. Its lower or moderate affinity may reduce the risk of hyperkalemia, which is a common side effect of taking spironolactone, an example of clinically utilized antagonist drug (Rakugi et al., 2020). Hyperkalemia is an adverse effect of the aldosterone activation inhibition. Aldosterone normally regulates sodium retention and potassium excretion, so a strong antagonist can inhibit this process, leading to decreased potassium excretion (Hundemer & Sood, 2021). Lastly, 9,12-octadecadienoic acid demonstrated the lowest binding affinity of –6.3 kcal/mol, suggesting that it may function as a partial antagonist. Its effectiveness and bioavailability should be further studied.

The results of the molecular docking indicate that the phytochemicals that exhibited strong binding affinities can show antagonistic activity with the mineralocorticoid receptor, suggesting a potential cardioprotective effect. Root-mean square deviation (RMSD) values assess and quantify the variation between the obtained docking orientation and the corresponding co-crystallized conformation of the ligand (Ramirez & Caballero, 2018). The lower RMSD values indicate that the docking poses show almost no deviation from reference conformation, suggesting high stability and reliability. Moreover, the antagonistic effects of such metabolites could potentially offer therapeutic benefits. Further analysis is needed to confirm its therapeutic effects and if these metabolites effectively block the mineralocorticoid activation, they may help in reducing hypertension, vascular dysfunction, cardiac fibrosis, and heart failure (Sica et al., 2015). Experimental studies are needed to further support the specificity and safety of the following metabolites and need to be compared with current MR antagonists to determine therapeutic viability.

PPAR-a (2ZNN) with phytochemicals of *Pleurotus ostreatus* (3931, 5280794, 457801, 53232)

Various interactions are observed between PPAR-a and the secondary metabolites of Pleurotus ostreatus. PPAR-a with 9,12-octadecadienoic acid has a –6.2 kcal/mol binding affinity, indicating a moderate interaction strength, and is weaker compared to the other complex that relied more on hydrogen bonding. This suggests that while the ligand can bind to the receptor, the affinity deficits to produce a stronger binding energy since stronger hydrogen bonds or other additional interactions are absent (Terefe & Ghosh, 2022). As such, the balance between hydrophobic and hydrogen bonding interactions modulate the strength of the receptor-ligand binding (Wu et al., 2024). The moderate binding interaction between PPAR-a and 9,12-octadecadienoic acid, while functional, may not pose as a good interaction when compared to the other complexes. More hydrogen bonds indicate that the interaction between the ligand and receptor is stronger (Arthur & Uzairu, 2016). The fact could be observed in PPAR-a with stigmasta-5,22-dien-3-ol possessing a binding affinity of –7.0 kcal/mol with 2 conventional hydrogen bonds from ASP432 and LYS429 and a singular alkyl bond in PRO357. This combination of hydrophobic and hydrogen interactions, overall contributes to the stability of the ligand-receptor complex (Yoshida et al., 2020). However, the complex with gamma-sitosterol despite possessing only alkyl hydrophobic bonds, is stronger than both 9,12-octadecadienoic acid and stigmasta-5,22-dien-3-ol with a –8.0 kcal/mol binding affinity. While enthalpic characteristics or type of bonds affect binding strength, the same holds true to their entropic or molecular flexibility characteristics that compensates for energy losses (Freire, 2009). PPAR-a is a nuclear receptor with a hydrophobic ligand-binding domain which favors rigid, lipophilic ligands like sterols. Considering that gamma-sitosterol, a sterol, is larger and bulkier than 9,12-octadecadienoic acid, a flexible fatty acid chain, it loses less conformational entropy which justifies the more favorable binding affinity despite the lack of hydrogen bond. Ultimately, it is with lovastatin that PPAR-a demonstrated the strongest affinity with a docking score of –9.0 kcal/mol. Amongst the secondary metabolites, the complex with lovastatin contained the most hydrogen bonds and is also simultaneously stabilized by its alkyl hydrophobic bonds. This fact alone is compatible with prior claims and explains the strength of the interaction.

Insulin receptor (4IBM) with phytochemicals of *Pleurotus ostreatus* (3931, 5280794, 457801, 53232)

The binding affinity of IR with 9,12-octadecadienoic acid is –5.3 kcal/mol. This suggests that binding energy is not quite that of strength and rigidity. This might be because of the unfavorable interactions within the ligand-receptor such as the bond with ASP1229 as the amino acid residue. As the nature of 9,12-octadecadienoic acid is that it is a linoleic acid, it would bind to a hydrophobic pocket within the receptor, which may influence the overall structure of the receptor. Further, it can induce conformational shifts or changes in membrane-bound receptors such as the insulin receptor, affecting its tyrosine kinase activity and its ability to interact with downstream signaling molecules. Similarly, allosteric changes may also be found, if 9,12-octadecadienoic acid binds with other binding sites resulting in the activation or inhibitor of certain receptor functions. Escribano et al. (2017), stated in their study that an alteration in the expression profile of IR or its dysregulation is detrimentally associated with certain pathologies such as cancer, obesity that might lead to diabetes mellitus and insulin resistance, and atherosclerosis. Otherwise, when the receptor's activity is enhanced, the phosphorylation of tyrosine triggers the P13K/Akt and MAPK pathway, which then would promote glucose uptake, lipid metabolism, and cell growth (Chen et al., 2019).

The quantity of bonds formed between the interactions IR and gamma-sitosterol help in the stabilization of the receptor-ligand complex by ensuring that the ligand fits well into the receptor, tightly at that. This contributes to the overall binding energy of the complex and the complementarity of its shapes. Further adding to the van der Waals interactions, a conventional hydrogen bond with aspartate at position 1150, and alkyl groups are present. Gamma-sitosterol is a hydrophobic molecule whose alkyl groups may interact with the hydrophobic residues of the receptor. This also contributes to the overall forces that hold the ligand to the receptor. The binding affinity of IR with gamma-sitosterol is –7.6 kcal/mol. This binding affinity is on the threshold of 'high', this must be because of the diverse bonds seen in the ligand-receptor interaction. Gamma-sitosterol inhibits obesity-induced insulin resistance through the downregulation of IKKβ/NF-κB and c-Jun-N-terminal kinase (JNK) signaling pathway which returns inflammatory events in the adipose tissue (Jayaraman et al, 2021). This consequently suggests that gamma-sitosterol increases the uptake of glucose by adipocytes, and it also stimulates adipogenesis (Chai et al., 2010). All these reasons combined suggest that gamma-sitosterol is a good candidate for drug design and development. For stigmasta-5,22-dien-3-ol, although the interaction has an unfavor-

able bump, the binding affinity of the insulin receptor with stigmasta-5,22-dien-3-ol is –8.5kcal/mol. This is because of the varying van der Waals bonds in the interaction; this 'negates' the effect of such relationships. Stigmasterol inhibits cholesterol synthesis by inhibiting sterol Δ24-reductase in human Caco-2 and HL-60 cell lines, reducing hepatic cholesterol levels (Batta et al., 2006), which consequently concerns the cardiovascular system.

The binding affinity of the ligand-receptor complex is –7.8 kcal/mol. This indicates a binding affinity that is strong and rigid. Studies show that lovastatin is like a "double-edged sword", which demonstrates both a beneficial and detrimental effect upon health and overall wellbeing. Lovastatin has been shown to block downstream pathway signaling by inhibiting the phosphorylation of the IRβ subunit (Delle Bovi et al., 2019). This inhibition is suggestive of the mechanism of the anti-mitogenic effect of lovastatin (Mcguire et al., 1994). Further, lovastatin reduces receptor tyrosine phosphorylation levels, which inhibits the insulin receptor from activating the Mitogen-Activated Protein Kinase (MAPK,) resulting in its inhibition (Xu et al., 1996). However, when MAPK is inactivated or inhibited, the MAPK cascade would not be able to (1) modulate cardiac hypertrophy in times of stress and immense pressure, (2) regulate cardiac remodelling after myocardial infarction, (3) modulate atherosclerotic lesions, and lastly, (4) promote the formation of neointima succeeding vascular injury (Muslin, 2009). However, lovastatin acts to lower blood cholesterol by upregulating hepatic low-density lipoprotein receptors (Wasim et al., 2022), which, if not done, would lead to insulin resistance. Therefore, according to Muscogiuri et al. (2014), even if studies suggest that lovastatin intake raises the risk for developing insulin resistance; the benefits outweigh the risk.

RMSD

The favorable RMSD values seen in Table 1–9 indicate that the docked ligands showed minimal deviation from their original conformations. According to Bell & Zhang (2019), such findings suggest stable ligand placement during docking simulations (Bell & Zhang, 2019).

Biological implications for cardiovascular disease management

Angiotensin II type 1 receptor regulates blood pressure by inducing an increase through vasoconstriction, stimulation of the sympathetic nervous system, renal activities, and increased aldosterone biosynthesis (Fyhrquist & Tikkanen, 1995). On this account, the strong binding of stigmasta-5,22-dien-3-ol and gamma-sitosterol being –10.2 and –10.1 kcal/mol, respectively could potentially make them inhibitors for the receptor and produce antihypertensive effects, which could be explored further. The presence of strong hydrophobic bonds with both compounds further support this claim, particularly with gamma-sitosterol having a conventional hydrogen bond, making it a strong candidate for further study.

Similarly, interactions with MGAM show potential implications in the regulation and metabolism of glucose. Stigmasterol has anti-inflammatory and antioxidant effects, which help mitigate oxidative stress and inflammation, both of which contribute to CVD progression (Bakrim et al., 2022). Its high binding affinity to MGAM suggests potential anti-alpha-glucosidase activity, regulating hyperglycemia. Gamma-sitosterol exhibited hypolipidemic properties, exerting low binding energy against key enzymes in cholesterol biosynthesis (Balamurugan et al., 2015). Its high binding affinity to MGAM suggests broad inhibitory potential. Lovastatin, an established HMG-CoA reductase inhibitor, also interacts with MGAM significantly, suggesting possible implications in glucose homeostasis alongside its well-known role in lipid metabolism (Biocca et al., 2015).

Beta-2 adrenergic receptor (ADRB2) had the strongest binding affinity with stigmasta-5,22-dien-3-ol because of the various bonds that took place in the interaction between the two. The binding affinity is listed to be –9.5 kcal/mol. It is shown that stigmasta-5,22-dien-3-ol exhibits its effect as an antidiabetic by ameliorating glucose transporter type 4 (GLUT4) translocation and decreasing insulin resistance, which consequently decreases fasting glucose, and induces β-cell regeneration (Nualkaew et al., 2015 as cited in Bakrim et al., 2022). Moreover, although indirectly, research by Alkuwayti (2023) presented stigmasta-5,22-dien-3-ol as a substance extracted from *Solenostemma argel* as having anti-*Staphylococcus aureus* biofilm activity. As *S. aureus* releases toxic shock syndrome toxin-1 (TSST-1), which triggers many cytokines as it is a superantigen by nature, TSST-1 causes leakage in endothelial cells (Mahon & Lehman, 2023). Kwiecinski & Horswill (2021) added that in addition to sepsis, *S. aureus* presence in the blood may result in endocarditis. Stigmasta-5,22-dien-3-ol holds influence in the maintenance and plausibly cures cardiovascular diseases through various methods.

The interaction of these ligands with angiotensin-converting enzymes suggests potential implications for cardiovascular health, especially in regulating blood pressure and lipid metabolism. The relatively weaker binding affinity of 9,12-octadecadienoic acid compared to the other ligands suggests that its potential as a natural ACE inhibitor may be limited. On the other hand, stigmasta-5,22-dien-3-ol's high binding affinity to ACE suggests potential cardioprotective properties through ACE inhibition (Messerli et al., 2018; Bakrim et al., 2022). Similarly, gamma-sitosterol has demonstrated anti-inflammatory and antihyperlipidemic effects that can benefit cardiovascular health (Balamurugan et al., 2015; Naikwadi et al., 2023), with its binding affinity to ACE (–9.3 kcal/mol) falling within a similar range, suggesting that it may exert inhibitory effects on multiple cardiovascular disease-related pathways. Lastly, lovastatin, an HMG-CoA reductase inhibitor, shows strong affinity with ACE, suggesting a dual role in targeting both the cholesterol pathways and the renin-angiotensin system (Biocca et al., 2015).

The mineralocorticoid receptor (MR) plays a significant role in fluid and electrolyte regulation and its activation results in pathological changes, including oxidative stress, fibrosis, and inflammation. Clinical and experimental studies utilize mineralocorticoid antagonists to preserve cardioprotective effects and manage cardiovascular conditions, such as arrhythmias, atherosclerosis, myocardial infarction, heart failure, and cardiovascular damage (Barrera-Chimal et al., 2022). A study of Bauersachs & López-Andrés (2021) underscores that, consistent with various cellular evidence, blocking the mineralocorticoid receptor by antagonists in disease models and genetically modified mice with cell-specific MR overexpression and deletion reinforces the protective role of MR antagonists in cardiovascular dysfunction. Given that the activation of mineralocorticoid receptors results in cardiovascular diseases, such as inflammation, fibrosis, and oxidative stress, the high binding affinity of the following metabolites indicates a possible mineralocorticoid receptor antagonist effect. This MR antagonist effect is similar to known antagonist drugs, including finerenone, eplerenone, and spironolactone (Malinowski & Jean, 2018; Georgianos & Agarwal, 2022). Mineralocorticoid receptors have long been a significant part of medical therapy for different cardiovascular conditions and various clinical trials confirmed the benefits of mineralocorticoid receptor antagonists as a treatment in managing cardiovascular disease.

Contrary to the effects of lovastatin on the IR and its downstream signaling pathways, stigmasta-5,22-dien-3-ol, on the other hand, promotes glucose uptake through the P13K pathway and serves as an insulin mimetic (Sujatha et al., 2010 as cited in Sangeetha et al., 2017). Going from this, the potential for the maintenance of insulin-related diseases such as type 2 diabetes mellitus is not far from development.

Glucocorticoid receptors are activated by endogenous steroid hormones or by exogenous glucocorticoids and act within the cardiovascular system, which then can influence the progress and prognosis of cardiovascular diseases (Liu et al., 2019). Additionally, Cruz-Topete et al. (2020) stated that glucocorticoids exert cardioprotective and anti-inflammatory effects and have an essential role in controlling blood pressure and cardiac function. The molecular docking analysis suggests that the weak interaction between glucocorticoid and the two ligands, 9,12-octadecadienoic acid and gamma-sitosterol, indicate a limited modulation of the receptor activity, affecting how the body processes lipids. On the other hand, the strong binding affinity with lovastatin, a known cholesterol-lowering drug, suggests that receptors

may influence cholesterol regulation and atherosclerosis prevention. Moreover, based on the docking results, the receptor prefers hydrophobic interactions, highlighting the potential of targeting it with non-polar drugs to achieve cardiovascular benefits.

HMG-CoA reductase is known as a lipid-lowering medication that is mainly used in the coronary heart disease prevention .It reviews the indications and mechanism of action of statins for the management of coronary heart disease and familial dyslipidemias (Bansal & Cassagnol, 2023). These statins are designed to reduce low-density lipoprotein (LDL) levels and completely inhibit HMG-CoA reductase, which is the rate limiting enzyme of the mevalonate pathway. Moreover, HMG-CoA reductase is principal and one of the effective drugs for the management of atherosclerotic vascular disease (Lutgens & Daemen, 2004). On the other hand, lovastatin increases miR-29b expression and decreases proteasome activity in human umbilical vein endothelial cells (HUVECs). The effect of lovastatin inhibits the oxidative stress which is induced by multiple oxidants such as ox-LDL, TNFa, and high glucose (HG) , which is reversed by the inhibition of miR-29 in HUVECs. The administration of lovastatin prevents the endothelial dysfunction in humans with hyperglycemia, dyslipidemia, and hyperhomocysteinemia (Wang et al., 2016).

In addition to that, peroxisome proliferator-activated receptor alpha (PPAR-α) regulates lipid metabolism, fatty acid oxidation, and inflammation (Montaigne et al., 2021). Activation of PPAR-α reduces triglyceride levels and increases high-density lipoprotein (HDL) cholesterol, making it a target for fibrate drugs in dyslipidemia treatment. The docking results indicate that stigmasta-5,22-dien-3-ol (–9.8 kcal/mol) and gamma-sitosterol (–9.6 kcal/mol) strongly interact with PPAR-α, potentially acting as agonists. The pi-alkyl and alkyl interactions suggest that this compound could promote lipid metabolism activation, reducing the risk of atherosclerosis and coronary artery disease. These findings support further exploration of *Pleurotus ostreatus* phytochemicals as natural lipid-lowering agents.

Absorption, distribution, metabolism, excretion, and toxicity prediction (ADMET)

Data reported from ADMET 3.0 LAB coupled with SwissAdme indicated that 9,12-octadecadienoic acid and lovastatin possessed high gastrointestinal absorption. This finding suggests efficient passage through the intestinal wall and further entry to the bloodstream when the drug dose is taken orally. These two compounds being lipophilic (Climent et al., 2021), likely contributed to the results since their passive diffusion allows readily crossing of lipid-rich cell membranes through the intestinal wall. In contrast, the low GI absorption of gamma-sitosterol and stigmasta-5,22-dien-3-ol could be attributed to their poor water solubility and high molecular weight. Supporting this finding are the reports from Bhalani et al. (2023) and Azman et al. (2022) indicating that poor water solubility or high molecular weight imposes difficulty in traveling through the intestinal membranes (Azman et al., 2022; Bhalani et al., 2023). Meanwhile, the high plasma protein binding of gamma-sitosterol (98.64%), 9,12-octadecadienoic acid (96.96%), and lovastatin (91.72%) suggest that a small fraction of the compound is available for active transport to target receptors. Although attributed by a longer duration of action, it may mean limited immediate bioavailability and hindrance to tissue penetration (Wanat, 2020; Onetto & Sharif, 2023). On the other hand, stigmasta-5,22-dien-3-ol exhibits moderate to low PPB of 86.31% and as per Keller et al. (1984) signifies higher proportions and activity of free drug available in circulation albeit faster clearance. Significantly, all compounds did not demonstrate blood-brain barrier permeability, contributing to potential CVD management as CNS side effects are unwanted.

Table 12 shows that gamma-sitosterol, lovastatin, and stigmasta-5,22-dien-3-ol are cytochrome P450 3A4 (CYP3A4) substrates. The finding shows these compounds to be dependent on the liver enzyme, CYP3A4 for systemic clearance (Mulder et al., 2021). By contrast, 9,12-octadecadienoic acid conforms to an alternative metabolic pathway. *Pleurotus ostreatus*' compounds that are CYP3A4 substrates signify variability from genetic differences and possible interferences from co-administered drugs that induce or inhibit CYP3A4 activity (Zhou et al., 2005; Klein & Zanger, 2013). In such instances, faster clearance or toxicity would occur if induced or inhibited, respectively. However, the lack of CYP3A4 inhibitors from the compounds other than lovastatin suggests non-interference with enzyme activity and low potential to slow other CYP3A4 drugs metabolism. Additionally, the human liver microsomal stability shows instability to gamma-sitosterol and stigmasta-5,22-dien-3-ol, requiring improvements for longer half-life and pharmacological effects while 9,12-octadecadienoic acid and lovastatin exert prolongation, not necessitating frequent dosing. Furthermore, distinct clearance rates and elimination pathways were expressed, contributing to their bioavailability and potential clinical applications. 9,12-octadecadienoic acid exhibited the lowest clearance rate with 3.80 mL/min/kg. This suggests a longer systemic duration by potentially enhancing pharmacological effects (Di & Obach, 2015). However, it increases accumulation risks in lipid-rich tissues. As anticipated, lovastatin delineated moderate clearance with 8.23 mL/min/kg, indicating a balanced therapeutic duration and safety. Meanwhile, gamma-sitosterol and stigmasta-5,22-dien-3-ol demonstrated rapid clearance of 12.68 and 13.92 mL/min/kg, respectively, portraying rapid clearance and efficient elimination, which reinforces further enhancements.

The selected phytochemicals of *P. ostreatus* demonstrated low inhibition of the human Ether-à-go-go-Related Gene (hERG) (Table 13). This proposes favorable data especially for potential cardiovascular treatment since it is not antagonistic to the intended effect, indicating that the phytochemicals are unlikely to cause significant cardiotoxic effects. Although in regards to hepatotoxicity, gamma-sitosterol, lovastatin, and stigmasta-5,22-dien-3-ol demonstrated the potential toxic effect, necessitating the need for further monitoring and optimization to minimize liver-related side effects. 9,12-octadecadienoic acid, on the other hand, does not exhibit hepatotoxicity, making it a relatively safer alternative for long-term use in relation to liver health. AMES mutagenicity predicts the carcinogenic potential of compounds (Vijay et al, 2018), in which all phytochemicals are shown to be unlikely to cause direct DNA mutations. This supports their suitability for therapeutic use without major concerns regarding genotoxicity.

Conclusion

This study was conducted to explore the therapeutic potential of the secondary metabolites of *Pleurotus ostreatus*: stigmasta-5,22-dien-3-ol, gamma-sitosterol, lovastatin, and 9,12-octadecadienoic acid on selected receptors associated with cardiovascular diseases through their binding affinities, molecular interactions, and pharmacokinetic assessments using *in-silico* methods. Particularly, the molecular binding, docking scores, RMSD, and structural characteristics from the results provided the stability of the receptor-ligand interaction, allowing the researchers to determine the phytochemicals' strength and weakness in interacting with the cardiovascular receptor.

Molecular dockings demonstrated that stigmasta-5,22-dien-3-ol exhibited the strongest binding affinity, followed by gamma-sitosterol, lovastatin, the reference drug, and 9,12-octadecadienoic acid averaging –8.74, –8.40, –8.13, and –6.0 kcal/mol, respectively, among the cardiovascular receptors: alpha-glucosidase, angiotensin-converting enzyme, beta-2 adrenergic receptor, HMG-CoA reductase, insulin receptor, mineralocorticoid receptor, PPAR-a, and text expression angiotensin II receptor. Notably, RMSD values of 0.0 Å were delineated by all phytochemicals, indicating that the docked ligands showed minimal deviation from their original conformations. Receptor-ligand interaction primarily exhibited hydrophobic bonds including pi-alkyl, alkyl-alkyl, and pi-sigma. This finding suggests an overall contribution to the stability of the complex, indicating their greater affinity with lipid environments. Following the numerous hydrophobic bonds are conventional hydrogen bonds from specific ligands with their respective receptors , which increases the specificity for the interaction, greatly complementing their therapeutic value. The consistently superior binding affinities of stigmasta-5,22-dien-3-ol and gamma-sitosterol, surpassing lovastatin, highlight their potential the-

rapeutic effects for cardiovascular diseases. These interactions suggest biological implications by theoretically possessing antihypertensive effects with AT1R and ACE, cholesterol and lipid regulation from inhibition of HMG-CoA reductase and activation of PPAR-α, blood pressure and fluid balance control for affinity with ADRB2 and mineralocorticoid, and anti-diabetic benefits with the insulin receptor and α-glucosidase. Potentially, these findings suggest *P. ostreatus* as a natural therapeutic for hypertension, dyslipidemia, and metabolic syndrome, warranting further development and confirmation through complementary studies.

ADMET profiling of the secondary metabolites of *P. ostreatus*: stigmasta-5,22-dien-3-ol, gamma-sitosterol, lovastatin, and 9,12-octadecadienoic acid provided an in-depth assessment of their pharmacokinetic properties, reinforcing their potential viability as cardiovascular disease therapeutics. Notably, lovastatin and 9,12-octadecadienoic acid exhibited high gastrointestinal absorption, suggesting better systemic bioavailability, while stigmasta-5,22-dien-3-ol and gamma-sitosterol demonstrated low absorption, potentially limiting their therapeutic effectiveness unless enhanced through formulation strategies. Plasma protein binding results indicated that all compounds displayed high affinity (>85%), affecting free drug availability in circulation. Additionally, none of the compounds showed blood-brain barrier permeability, minimizing risks of neurological side effects and ensuring cardiovascular specificity. Metabolic predictions indicated that lovastatin, stigmasta-5,22-dien-3-ol, and gamma-sitosterol are CYP3A4 substrates, suggesting that they undergo hepatic metabolism, whereas 9,12-octadecadienoic acid follows a non-CYP3A4 pathway, potentially extending its systemic duration. Excretion results imply that gamma-sitosterol and stigmasta-5,22-dien-3-ol are rapidly cleared, indicating shorter systemic exposure, while 9,12-octadecadienoic acid had the lowest clearance, contributing to a longer circulation time but raising potential accumulation concerns. Meanwhile, toxicity assessments confirmed that none of the compounds exhibited strong mutagenic or carcinogenic risks, with lovastatin showing moderate hepatotoxicity, necessitating controlled dosing.

Based on these parameters, the researchers evaluated each ligand's therapeutic viability. Lovastatin exhibited the most balanced ADMET characteristics, maintaining moderate clearance, high bioavailability, and well-established metabolism, reinforcing its clinical relevance as a reference drug. Stigmasta-5,22-dien-3-ol and gamma-sitosterol, while demonstrating strong receptor binding, require pharmacokinetic optimization to overcome poor absorption and rapid clearance. However, their high plasma protein binding affinity and extensive hydrophobic interactions suggest strong lipid solubility, which could contribute to their efficacy in modulating lipid metabolism and cholesterol regulation. Meanwhile, the prolonged systemic presence of 9,12-octadecadienoic acid suggests sustained cardiovascular effects but necessitates further investigation to assess long-term safety for mitigating potential accumulation risks. These findings emphasize the challenges in balancing strong receptor binding with optimal pharmacokinetic properties, a key hurdle in drug development. Incorporating both computational ADMET analysis and molecular docking reinforces their therapeutic potential. Ultimately, this study underscores the potential of *P. ostreatus*' secondary metabolites as natural alternatives for cardiovascular disease management, provided that their pharmacokinetic limitations are addressed.

We thank Far Eastern University – Manila, Department of Medical Technology, the Institute of Health Sciences and Nursing.

The authors declare that they have no known competing financial interests or personal relationships that could have appeared to influence the work reported in this paper.

This research did not receive any specific grant from funding agencies in the public, commercial, or non-profit sectors.

References

Alkuwayti, M. A. (2023). Anti-*Staphylococcus aureus* activity of the aqueous ethanolic extract of *Solenostemma* argel aerial parts. Journal of Pure and Applied Microbiology, 17(4), 2581.

Alum, E. U. (2024). Role of phytochemicals in cardiovascular disease management: Insights into mechanisms, efficacy, and clinical application. Phytomedicine Plus, 5(1), 100695.

Arthur, D. E., & Uzairu, A. (2019). Molecular docking studies on the interaction of NCI anticancer analogues with human phosphatidylinositol 4,5-bisphosphate 3-kinase catalytic subunit. Journal of King Saud University – Science, 31(4), 1151–1166.

Azman, M., Sabri, A. H., Anjani, Q. K., Mustaffa, M. F., & Hamid, K. A. (2022). Intestinal absorption study: Challenges and absorption enhancement strategies in improving oral drug delivery. Pharmaceuticals, 15(8), 975.

Bakrim, S., Benkhaira, N., Bourais, I., Benali, T., Lee, L.-H., El Omari, N., Sheikh, R. A., Goh, K. W., Ming, L. C., & Bouyahya, A. (2022). Health benefits and pharmacological properties of stigmasterol. Antioxidants, 11(10), 1912.

Balamuragan, R., Stalin, A., Aravinthan, A., & Kim, J. (2015). Sitosterol a potent hypolipidemic agent: *In silico* docking analysis. Medicinal Chemistry Research, 24, 124–130.

Balamurugan, R., Duraipandiyan, V., & Ignacimuthu, S. (2011). Antidiabetic activity of γ-sitosterol isolated from *Lippia nodiflora* L. in streptozotocin induced diabetic rats. European Journal of Pharmacology, 667, 410–418.

Barratt, E., Bingham, R. J., Warner, D. J., Laughton, C. A., Phillips, S. E. V., & Homans, S. W. (2005). Van der Waals interactions dominate ligand–protein association in a protein binding site occluded from solvent water. Journal of the American Chemical Society, 127(33), 11827–11834.

Barrera-Chimal, J., Bonnard, B., & Jaisser, F. (2022). Roles of mineralocorticoid receptors in cardiovascular and cardiorenal diseases. Annual Review of Physiology, 84(1), 585–610.

Batta, A. K., Xu, G., Honda, A., Miyazaki, T., & Salen, G. (2006). Stigmasterol reduces plasma cholesterol levels and inhibits hepatic synthesis and intestinal absorption in the rat. Metabolism, 55(3), 292–299.

Bauersachs, J., & López-Andrés, N. (2021). Mineralocorticoid receptor in cardiovascular diseases – Clinical trials and mechanistic insights. British Journal of Pharmacology, 179(13), 3119–3134.

Beach, M., Davey, T., Subramanian, P., & Such, G. (2023). Self-healing organic coatings – Fundamental chemistry to commercial application. Progress in Organic Coatings, 183, 107759.

Bell, E. W., & Zhang, Y. (2019). DockRMSD: An open-source tool for atom mapping and RMSD calculation of symmetric molecules through graph isomorphism. Journal of Cheminformatics, 11, 40.

Bhalani, D. V., Nutan, B., Kumar, A., & Singh Chandel, A. K. (2022). Bioavailability enhancement techniques for poorly aqueous soluble drugs and therapeutics. Biomedicines, 10(9), 2055.

Biocca, S., Iacovelli, F., Matarazzo, S., Vindigni, G., Oteri, F., Desideri, A., & Falconi, M. (2015). Molecular mechanism of statin-mediated LOX-1 inhibition. Cell Cycle, 14(10), 1583–1595.

Boora, P., Puri, R., Rani, S., & Mehta, M. (2023). Effects of *Meconopsis aculeata* royle extracts on leukocytosis and eosinophilia induced by milk in albino mice: Anti-asthmatic property. Journal of Scientific Research, 15(3), 819–830.

Bulusu, G., & Desiraju, G. R. (2019). Strong and weak hydrogen bonds in protein–ligand recognition. Journal of the Indian Institute of Science, 100(1), 31–41.

Chai, J., Ling, S., Kanthimathi, M. S., & Kuppusamy, U. R. (2010). Gene regulation in β-sitosterol-mediated stimulation of adipogenesis, glucose uptake, and lipid mobilization in rat primary adipocytes. Genes and Nutrition, 6, 181–188.

Chen, J., Huang, L., Qi, X., & Chen, C. (2019). Insulin receptor trafficking: Consequences for insulin sensitivity and diabetes. International Journal of Molecular Science, 20(20), 5007.

Climent, E., Benaiges, D., & Pedro-Botet, J. (2021). Hydrophilic or lipophilic stains? Frontiers in Cardiovascular Medicine, 8, 687585.

Cramer, D. L., Cheng, B., Tian, J., Clements, J. H., Wypych, R. M., & Martin, S. F. (2020). Some thermodynamic effects of varying nonpolar surfaces in protein-ligand interactions. European Journal of Medicinal Chemistry, 208, 112771.

Cruz-Topete, D., Oakley, R. H., & Cidlowski, J. A. (2020). Glucocorticoid signaling and the aging heart. Frontiers in Endocrinology, 11, 347.

Cuenca-Bermejo, L., Almela, P., Navarro-Zaragoza, J., Villalba, E. F., Gonzalez-Cuello, A., Laorden, M., & Herrero, A. (2021). Cardiac changes in Parkinson's disease: Lessons from clinical and experimental evidence. International Journal of Molecular Sciences, 22(24), 13488.

De Denus, S., & Spinler, S. A. (2002). Early statin therapy for acute coronary syndromes. The Annals of Pharmacotherapy, 36(11), 1749–1758.

Delle Bovi, R. J., Kim, J., Suresh, P., London, E., & Miller, W. T. (2019). Sterol structure dependence of insulin receptor and insulin-like growth factor 1 receptor activation. Biochimica et Biophysica Acta – Biomembranes, 1861(4), 819–826.

Dhorajiwala, T., Halder, S., & Samant, L. (2019). Comparative *in silico* molecular docking analysis of L-threonine-3-dehydrogenase, a protein target

against African trypanosomiasis using selected phytochemicals. Journal of Applied Biotechnology Reports, 6(3), 101–108.
Di Cesare, M., Perel, P., Taylor, S., Kabudula, C., Bixby, H., Gaziano, T. A., McGhie, D. V., Mwangi, J., Pervan, B., Narula, J., Pineiro, D., & Pinto, F. J. (2024). The heart of the world. Global Heart, 19(1), 11.
Di, L., & Obach, R. S. (2015). Addressing the challenges of low clearance in drug research. The AAPS Journal, 17(2), 352–357.
Duong, H., & Bajaj, T. (2025). Lovastatin. StatPearls, Treasure Island.
Endrini, S., Rahmat, A., Ismail, P., & Tafuiq-Yap, Y. H. (2014). Cytotoxic effect of γ-sitosterol from kejibeling (*Strobilanthes crispus*) and its mechanism of action towards *c-myc* gene expression and apoptotic pathway. Medical Journal of Indonesia, 23(4), 203–208.
Escribano, O., Beneit, N., Rubio-Longas, C., Lopez-Pastor, A. R., & Gomez-Hernandez, A. (2017). The role of insulin receptor isoforms in diabetes and its metabolic and vascular complications. Journal of Diabetes Research, 2017, 1403206.
Farvid, M. S., Ding, M., Pan, A., Sun, Q., Chiuve, S. E., Steffen, L. M., Willett, W. C., & Hu, F. B. (2014). Dietary linoleic acid and risk of coronary heart disease: A systematic review and meta-analysis of prospective cohort studies. Circulation, 130(18), 1568–1578.
Ferenczy, G. G., & Kellermayer, M. (2022). Contribution of hydrophobic interactions to protein mechanical stability. Computational and Structural Biotechnology Journal, 20, 1946–1956.
Freire, E. (2009). A thermodynamic approach to the affinity optimization of drug candidates. Chemical Biology and Drug Design, 74(5), 468–472.
Fu, Y., Zhao, J., & Chen, Z. (2018). Insights into the molecular mechanisms of protein-ligand interactions by molecular docking and molecular dynamics simulation: A case of oligopeptide binding protein. Computational and Mathematical Methods in Medicine, 2018, 3502514.
Fyhrquist, F., Metsärinne, K., & Tikkanen, I. (1995). Role of angiotensin II in blood pressure regulation and in the pathophysiology of cardiovascular disorders. Journal of Human Hypertension, 9(S5), S19–S24.
Garzon-Siatoya, W. T., Carrillo-Martin, I., Chiarella, S. E., & Gonzalez-Estrada, A. (2021). State-of-the-art beta-adrenoreceptor agonists for the treatment of asthma. Expert Opinion on Pharmacotherapy, 23(2), 243–254.
Gelosa, P., Cimino, M., Pignieri, A., Tremoli, E., Guerrini, U., & Sironi, L. (2007). The role of HMG-CoA reductase inhibition in endothelial dysfunction and inflammation. Vascular Health and Risk Management, 3(5), 567–577.
Georgianos, P. I., & Agarwal, R. (2022). The nonsteroidal mineralocorticoid-receptor-antagonist finerenone in cardiorenal medicine: A state-of-the-art review of the literature. American Journal of Hypertension, 36(3), 135–143.
Grosu, L., Grosu, A. I., Crisan, D., Zlibut, A., & Perju-Dumbrava, L. (2023). Parkinson's disease and cardiovascular involvement: Edifying insights (review). Biomedical Reports, 18(3), 25.
Hamedi, A., Sakhteman, A., & Moheimani, S. M. (2020). An *in silico* approach towards investigation of possible effects of essential oils constituents on receptors involved in cardiovascular diseases (CVD) and associated risk factors (diabetes mellitus and hyperlipidemia). Cardiovascular and Hematological Agents in Medicinal Chemistry, 19(1), 32–42.
Hundemer, G. L., & Sood, M. M. (2021). Hyperkalemia with RAAS inhibition: Mechanism, clinical significance, and management. Pharmacological Research, 172, 105835.
Jayaraman, S., Devarajan, N., Rajagopal, P., Babu, S., Ganesan, S. K., Veeraraghavan, V. P., Palanisamy, C. P., Cui, B., Periyasamy, V., & Chandrasekar, K. (2021). β-Sitosterol circumvents obesity induced inflammation and insulin resistance by down-regulating IKKβ/NF-κB and JNK signaling pathway in adipocytes of type 2 diabetic rats. Molecules, 26(7), 2101.
Jhund, P. S., Talebi, A., Henderson, A. D., Claggett, B. L., Vaduganathan, M., Desai, A. S., Lam, C. S. P., Pitt, B., Senni, M., Shah, S. J., Voors, A. A., Zannad, F., Solomon, S. D., & McMurray, J. J. V. (2024). Mineralocorticoid receptor antagonists in heart failure: An individual patient level meta-analysis. The Lancet, 404(10458), 1119–1131.
Jimenez, J., & Benitez, M. J. (2024). Gibbs free energy and enthalpy-entropy compensation in protein-ligand interactions. Biophysica, 4(2), 21.
Kadam, P., Yadav, K., Karanje, A., Giram, D., Mukadam, R., & Patil, M. (2023). The food and medicinal benefits of oyster mushroom (*Pleurotus ostreatus*): A review. International Journal of Pharmaceutical Sciences and Research, 14(2), 883–890.
Keller, F., Maiga, M., Neumayer, H. H., Lode, H., & Distler, A. (1984). Pharmacokinetic effects of altered plasma protein binding of drugs in renal disease. European Journal of Drug Metabolism and Pharmacokinetics, 9(3), 275–282.
Kemp, B. E., Mitchelhill, K. I., Stapleton, D., Michell, B. J., Chen, Z., & Witters, L. A. (2022). Dealing with energy demand: The AMP-activated protein kinase. Trends in Biochemical Sciences, 24(1), 22–25.
Klein, K., & Zanger, U. M. (2013). Pharmacogenomics of cytochrome P_{450} 3A4: Recent progress toward the "missing heritability" problem. Frontiers in Genetics, 4, 12.
Kwiecinski, J. M., & Horswill, A. R. (2021). *Staphylococcus aureus* bloodstream infections: Pathogenesis and regulatory mechanisms. Current Opinion in Microbiology, 53, 51–60.
Liu, B., Zhang, T., Knight, J. K., & Goodwin, J. E. (2019). The glucocorticoid receptor in cardiovascular health and disease. Cells, 8(10), 1227.
Lutgens, E., & Daemen, M. J. (2004). HMG-coA reductase inhibitors: Lipid-lowering and beyond. Drug Discovery Today Therapeutic Strategies, 1(2), 189–194.
Mahon, C. R., & Lehman, D. C. (2023). Textbook of diagnostic microbiology. 7th ed. Elsevier.
Majewski, M., Ruiz-Carmona, S., & Barril, X. (2019). An investigation of structural stability in protein-ligand complexes reveals the balance between order and disorder. Communications Chemistry, 2, 110.
Malinowski, J. T., & Jean Jr., D. J. S. (2018). Next-generation small molecule therapies for heart failure: 2015 and beyond. Bioorganic and Medicinal Chemistry Letters, 28(9), 1429–1435.
Mcguire, T. F., Xu, X. Q., Corey, S. J., Romero, G. G., & Sebti, S. M. (1994). Lovastatin disrupts early events in insulin signaling: A potential mechanism of lovastatins anti-mitogenic activity. Biochemical and Biophysical Research Communication, 204(1), 399–406.
Messerli, F. H., Bangalore, S., Bavishi, C., & Rimoldi, S. F. (2018). Angiotensin-converting enzyme inhibitors in hypertension: To use or not to use? Journal of the American College of Cardiology, 71(13), 1474–1482.
Mishra, V., Tomar, S., Yadav, P., Vishwakarma, S., & Singh, M. P. (2022). Elemental analysis, phytochemical screening and evaluation of antioxidant, antibacterial and anticancer activity of *Pleurotus ostreatus* through *in vitro* and *in silico* approaches. Metabolites, 12(9), 821.
Montaigne, D., Butruille, L., & Staels, B. (2021). PPAR control of metabolism and cardiovascular functions. Nature Reviews Cardiology, 18(12), 809–823.
Mulder, T. A. M., van Eerden, R. A. G., de With, M., Elens, L., Hesselink, D. A., Matic, M., Bins, S., Mathijssen, R. H. J., & van Schaik, R. H. N. (2021). CYP3A4*22 genotyping in clinical practice: Ready for implementation? Frontiers in Genetics, 12, 711943.
Muscogiuri, G. Sarno, G., Gastaldelli, A., Savastano, S., Ascione, A., Colao, A., & Orio, F. (2014). The good and bad effects of statins on insulin sensitivity and secretion. Endocrine Research, 4, 137–143.
Muslin, A. J. (2008). MAPK signalling in cardiovascular health and disease: molecular mechanisms and therapeutic targets. Clinical Science, 115(7), 203–218.
Naikwadi, P. H., Mane, D. V., & Phatangre, N. (2023). Active anti-inflammatory potency of γ-sitosterol from *Woodfordia floribunda* Salisb. The Journal of Plant Science Research, 38(2), 691–700.
Nishiyama, A. (2018). Pathophysiological mechanisms of mineralocorticoid receptor-dependent cardiovascular and chronic kidney disease. Hypertension Research, 42(3), 293–300.
Odhar, H. A., Hashim, A. F., & Humad, S. S. (2022). Molecular docking analysis and dynamics simulation of salbutamol with the monoamine oxidase B (MAO-B) enzyme. Bioinformation, 18(3), 304–309.
Onetto, A. J., Sharif, S. (2023). Drug distribution. StatPearls, Treasure Island.
Patil, R., Das, S., Stanley, A., Yadav, L., Sudhakar, A., & Varma, A. K. (2010). Optimized hydrophobic interactions and hydrogen bonding at the target-ligand interface leads the pathways of drug-designing. PLoS One, 5(8), e12029.
Piska, K., Sułkowska-Ziaja, K., & Muszyńska, B. (2017). Edible mushroom *Pleurotus ostreatus* (oyster mushroom) – its dietary significance and biological activity. Acta Scientiarum Polonorum Hortorum Cultus, 16(1), 151–161.
Rakugi, H., Yamakawa, S., & Sugimoto, K. (2020). Management of hyperkalemia during treatment with mineralocorticoid receptor blockers: Findings from esaxerenone. Hypertension Research, 44(4), 371–385.
Ramírez, D., & Caballero, J. (2018). Is it reliable to take the molecular docking top scoring position as the best solution without considering available structural data? Molecules, 23(5), 1038.
Ray, K. K., & Cannon, C. P. (2005). The potential relevance of the multiple lipid-independent (pleiotropic) effects of statins in the management of acute coronary syndromes. Journal of the American College of Cardiology, 46(8), 1425–1433.
Righetti, P. G., & Boschetti, E. (2013). Low-abundance protein access by combinatorial peptide libraries. In: Righetti, P. G., & Boschetti, E. (Eds.). Low-abundance proteome discovery. Elsevier. Pp. 79–157.
Roth, C., Neal, B., & Lenhoff, A. (2000). Van der Waals interactions involving proteins. Biophysical Journal, 70(2), 977–987.
Sangeetha, K. N., Sujatha, S., Muthusamy, V. S., Anand, S., Shilpa, K., Kumari, P. J., Sarathkumar, B., Thiyagarajan, G., & Lakshmi, B. S. (2017). Current trends in small molecule discovery targeting key cellular signaling events towards the combined management of diabetes and obesity. Bioinformation, 13(12), 394–399.
Shao, C., Wang, J., Tian, J., & Tang, Y. (2020). Coronary artery disease: From mechanism to clinical practice. In: Wang, M. (Ed.). Coronary artery disease: Therapeutics and drug discovery. Springer, Singapore. Pp. 1–36.

Sica, D. A. (2015). Mineralocorticoid receptor antagonists for treatment of hypertension and heart failure. Methodist DeBakey Cardiovascular Journal, 11(4), 235.
Sim, L., Quezada-Calvillo, R., Sterchi, E. E., Nichols, B. L., & Rose, D. R. (2008). Human intestinal maltase – glucoamylase: Crystal structure of the N-terminal catalytic subunit and basis of inhibition and substrate specificity. Journal of Molecular Biology, 375(3), 782–792.
Sirikhansaeng, P., Tanee, P., Sudmoon, R., & Chaveerach, A. (2017). Major phytochemical as γ-sitosterol disclosing and toxicity testing in *Lagerstroemia* species. Evidence-Based Complementary and Alternative Medicine, 2017, 7209851.
Srivastava, S., Sahin, M., & Prock, L. (2019). Translational medicine strategies in drug development for neurodevelopmental disorders. Handbook of Behavioral Neuroscience, 29, 309–331.
Sujatha, S., Anand, S., Sangeetha, K. N., Shilpa, K., Lakshmi, J., Balakrishnan, A., & Lakshmi, B. S. (2010). Biological evaluation of (3β)-stigmast-5-en-3-ol as potent anti-diabetic agent in regulating glucose transport using in vitro model. International Journal of Diabetes Mellitus, 2(2), 101–109.
Tatulian, S. A. (2015). Structural dynamics of insulin receptor and transmembrane signaling. Biochemistry, 54(36), 5523–5532.
Terefe, E. M., & Ghosh, A. (2022). Molecular docking, validation, dynamics simulations, and pharmacokinetic prediction of phytochemicals isolated from croton dichogamus against the HIV-1 reverse transcriptase. Bioinformatics and Biology Insights, 16, 11779322221125605.
Tripathi, N., Kumar, S., Singh, R., Singh, C. J., Singh, P., & Varshney, V. (2013). Isolation and identification of gamma-sitosterol by GC-MS from roots of *Girardinia heterophylla*. Oriental Journal of Chemistry, 29(2), 705–707.
Uzzaman, M., Chowdhury, M. K., & Hossen, M. B. (2019). Thermochemical, molecular docking and ADMET studies of Aspirin metabolites. Frontiers in Drug Chemistry and Clinical Research, 2(3), 1–5.
Vaidyanathan, R., Sreedevi, S. M., Ravichandran, K., Vinod, S. M., Krishnan, Y. H., Babu, L. K., Parthiban, P. S., Basker, L., Perumal, T., Rajaraman, V., Arumugam, G., Rajendran, K., & Mahalingam, V. (2023). Molecular docking approach on the binding stability of derivatives of phenolic acids (DPAs) with human serum albumin (HSA): Hydrogen-bonding versus hydrophobic interactions or combined influences? JCIS Open, 12, 100096.
Vijay, U., Gupta, S., Mathur, P., Suravajhala, P., & Bhatnagar, P. (2018). Microbial mutagenicity assay: AMES Test. Bio-Protocol, 8(6), 1–15.
Waktola, G., & Temesgen, T. (2020). Pharmacological activities of oyster mushroom (*Pleurotus ostreatus*). Novel Research in Microbiology Journal, 4(2), 688–695.
Wanat, K. (2020). Biological barriers, and the influence of protein binding on the passage of drugs across them. Molecular Biology Reports, 47, 3221–3231.
Wang, C. C. L., Hess, C. N., Hiatt, W. R., & Goldfine, A. B. (2016). Clinical update: Cardiovascular disease in diabetes mellitus. Circulation, 133(24), 2459–2502.
Wang, J., Liang, J., Chen, L., Zhang, W., Kong, L., Peng, C., Su, C., Tang, Y., Deng, Z., & Wang, Z. (2021). Structural basis for the biosynthesis of lovastatin. Nature Communications, 12, 867.
Wangchuk, P. (2018). Therapeutic applications of natural products in herbal medicines, biodiscovery programs, and biomedicine. Journal of Biologically Active Products from Nature, 8(1), 1–20.
Wasim, R., Ansari, T. M., Ahsan, F., Siddiqui, M. H., Singh, A., Shariq, M., & Parveen, S. (2022). Pleiotropic benefits of statins in cardiovascular diseases. Drug Research, 72(9), 477–486.
Wright, K. M., DiNapoli, S. R., Miller, M. S., Aitana Azurmendi, P., Zhao, X., Yu, Z., Chakrabarti, M., Shi, W., Douglass, J., Hwang, M. S., Han-Chung Hsiue, E., Mog, B. J., Pearlman, A. H., Paul, S., Konig, M. F., Pardoll, D. M., Bettegowda, C., Papadopoulos, N., Kinzler, K. W., Vogelstein, B., Zhou, S., & Gabelli, S. B. (2023). Hydrophobic interactions dominate the recognition of a KRAS G12V neoantigen. Nature Communication, 14, 5063.
Wu, M., Dai, D., & Yan, H. (2012). PRL-dock: Protein -ligand docking based on hydrogen bond matching and probabilistic relaxation labeling. Proteins Structure Function and Bioinformatics, 80(9), 2137–2153.
Wu, N., Zhang, R., Peng, X., Fang, L., Chen, K., & Jestila, J. S. (2024). Elucidation of protein–ligand interactions by multiple trajectory analysis methods. Physical Chemistry Chemical Physics, 26, 6903.
Xie, L., Zhu, G., Shang, J., Chen, X., Zhang, C., Ji, X., Zhang, Q., & Wei, Y. (2021). An overview on the biological activity and anti-cancer mechanism of lovastatin. Cellular Signalling, 87, 110122.
Xu, X. Q., McGuire, T. F., Blaskovich, M. A., Sebti, S. M., & Romero, G. (1996). Lovastatin inhibits the stimulation of mitogen-activated protein kinase by insulin in HIRcB fibroblasts. Archives of Biochemistry and Biophysics, 326(2), 233–237.
Yang, X., Zhao, T., Feng, L., Shi, Y., Jiang, J., Liang, S., Sun, B., Xu, Q., Duan, J., & Sun, Z. (2019). PM2.5-induced ADRB2 hypermethylation contributed to cardiac dysfunction through cardiomyocytes apoptosis via PI3K/Akt pathway. Environment International, 127, 601–614.
Yazdi, S., Stein, M., Elinder, F., Andersson, M., & Lindahl, E. (2016). The molecular basis of polyunsaturated fatty acid interactions with the shaker voltage-gated potassium channel. Computational Biology, 12(1), e1004704.
Yoshida, T., Oki, H., Doi, M., Fukuda, S., Yuzuriha, T., Tabata, R., Ishimoto, K., Kawahara, K., Ohkubo, T., Miyachi, H., Doi, T., & Tachibana, K. (2020). Structural basis for PPARα activation by 1H-pyrazolo-[3,4-b]pyridine derivatives. Scientific Reports, 10(1), 7623.
Zhang, H., Unal, H., Desnoyer, R., Han, G. W., Patel, N., Katritch, V., Karnik, S. S., Cherezov, V., & Stevens, R. C. (2015). Structural basis for ligand recognition and functional selectivity at angiotensin receptor. Journal of Biological Chemistry, 290(49), 29127–29139.
Zhao, D. (2021). Epidemiological features of cardiovascular disease in Asia. JACC: Asia, 1(1) 1–13.
Zhao, Q., Liu, X., Cui, L., & Ma, C. (2024). Extraction and bioactivities of the chemical composition from *Pleurotus ostreatus*: A review. Journal of Future Foods, 4(2), 111–118.
Zhou, S., Yung Chan, S., Cher Goh, B., Chan, E., Duan, W., Huang, M., & McLeod, H. L. (2005). Mechanism-based inhibition of cytochrome P_{450} 3A4 by therapeutic drugs. Clinical Pharmacokinetics, 44(3), 279–304.